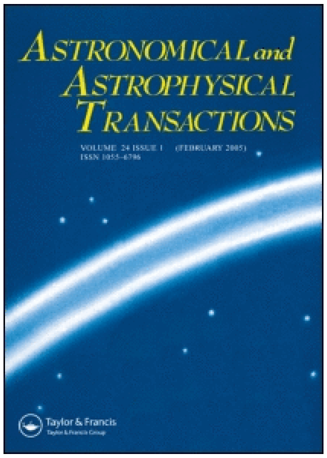

Astronomical & Astrophysical Transactions
The Journal of the Eurasian Astronomical Society
Publication details, including instructions for authors and subscription information:
http://www.informaworld.com/smpp/title~content=t713453505

Two-colour CCD imaging of 15 Seyfert galaxies. Observations

V. L. Afanasiev [a]; V. P. Mikhailov [a]; A. I. Shapovalova [a]
[a] State Scientific Center Special Astrophysical Observatory of the Russian Academy of Science, Karachaevo-Cherkesskaya Republic, Russia

Online Publication Date: 01 May 1998
To cite this Article: Afanasiev, V. L., Mikhailov, V. P. and Shapovalova, A. I. (1998) 'Two-colour CCD imaging of 15 Seyfert galaxies. Observations', Astronomical & Astrophysical Transactions, 16:4, 257 - 289
To link to this article: DOI: 10.1080/10556799808208159
URL: http://dx.doi.org/10.1080/10556799808208159

Astronomical and Astrophysical Transactions, 1998,
Vol. 16, pp. 257–289
Reprints available directly from the publisher
Photocopying permitted by license only

TWO-COLOUR CCD IMAGING OF 15 SEYFERT GALAXIES. OBSERVATIONS

V. L. AFANASIEV, V. P. MIKHAILOV, and A. I. SHAPOVALOVA

State Scientific Center Special Astrophysical Observatory of the Russian Academy of Science, 357147, N. Arkhyz, Karachaevo-Cherkesskaya Republic, Russia

(Received May 20, 1997)

We present the results of V (Johnson) and I/R (Cousins) CCD imaging of 15 Seyfert galaxies. Grey–scale and contour maps are provided as well as the results of elliptical fits to isophotes. The position angles and the axial ratios of the bars and the outer isophotes are obtained for each galaxy. We have found one clear and one possible unidentified bar, four inner and two outer rings in the galaxies not previously classified as barred or having these rings. The presence of four bars, and one outer ring has been confirmed for the galaxies with uncertain classification. Three galaxies previously classified as having inner rings did not reveal these. Four multiple-barred galaxies have been found. Two of them clearly show a secondary bar within a primary bar and another two have been classified as possible double-barred galaxies. The bar orientations have been compared with the [OIII] and radio major axes for five galaxies with known [OIII] and radio maps. It has been determined that the bar is aligned with the [OIII] and radio emission in three objects. In the inner regions of Mkn 3, Mkn 573 and Mkn 1073 colour maps have revealed jet-like structures which are similar (for Mkn 3 and Mkn 573) to the [OIII] images on the same scale and have position angles close to those of the radio sources.

KEY WORDS Seyfert galaxies, structure of galaxies, photometry of galaxies

1 INTRODUCTION

The investigation of the large–scale luminous mass distribution in Seyfert galaxies and the study of the relationship between the nuclear activity and properties of host galaxies are important for understanding the origin and evolution active galactic nuclei.

The strong tendency for Seyfert galaxies to associate with spiral galaxies has been known for some time. It has been found that nearly all Seyferts have a spiral morphology (Adams, 1977; MacKenty, 1990; Granato *et al.*, 1993; Moles *et al.*, 1995). A number of authors have examined the surface brightness distribution to compare properties of Seyfert host galaxies with those of normal galaxies of the same morphological type. They concluded that colours, magnitudes and disk parameters of Seyferts are generally similar to those of spiral galaxies without active nuclei (Yee, 1983; MacKenty, 1990; Granato *et al.*, 1993).

Detailed morphological studies do not show a similar agreement. Simkin *et al.* (1980) found a significant excess of bars and outer rings among Seyferts with respect to their control sample of normal spirals. But recent surveys based on CCD images show that the fraction of barred spirals among Seyferts is the same as that found in normal galaxies (MacKenty, 1990; McLeod and Rieke, 1995). Moreover, MacKenty (1990) concluded that Seyfert galaxies nearly always have a bar or external perturbation as the fuel supply mechanism for their nuclei; and Moles *et al.* (1995) and Márquez (1996) determined that all the isolated active galaxies show the presence of non-axisymmetric perturbations such as bars and/or rings. On the contrary, McLeod and Rieke (1995) in a near-IR survey concluded that these mechanisms are not identified clearly in the large–scale luminous mass distribution in Seyferts.

Since bars in Seyfert galaxies might play a key role in the transportation of gas toward the nucleus (Simkin *et al.*, 1980; Shlosman *et al.*, 1989) the examination of the relationship between the non-axisymmetric perturbation and circumnuclear gas properties could be useful for finding observational manifestations of nucleus-feeding mechanisms. For example, in a study of sample of 19 Seyfert galaxies with published images and FWHM [OIII] Mikhailov (1986) has found a strong correlation between the [OIII] emission-line width and the bar orientation with respect to the line of sight. This result implies that the kinematic properties of the circumnuclear emission-line gas are determined by the non-axisymmetric gravitational potential of the bar.

It has been known for some time that the circumnuclear emission–line gas has a strong tendency to be aligned with radio continuum sources on the hundreds of parsecs scale (Haniff *et al.*, 1988; Wilson *et al.*, 1988). The generally accepted interpretation for this effect is a combination of the radio ejecta and the collimation of the nuclear ionizing radiation along the radio axis (Wilson *et al.*, 1988). An alternative scheme explains this effect as a manifestation of the gas motion over the non-axisymmetric gravitational potential field (Afanasiev *et al.*, 1987). Some observational kinematic and morphological features of the circumnuclear emission–line gas were explained in accordance with this scenario for ten Seyfert galaxies (Afanasiev and Sil'chenko, 1991, I–VI).

In this way it could be expected that a significant relationship between the orientation of the bar and the radio axis in Seyfert galaxies exists. A similar correlation for the [OIII] emission–line gas can take place as well. Bower *et al.* (1995) found that there is no strong tendency for bars and radio sources in Seyferts to be aligned, but their sample consisted of only eight galaxies. To determine if the suggested scenario might apply to Seyferts it is necessary to analyse a large sample of galaxies.

For these reasons, we decided to image in two bands a full sample of northern Seyfert galaxies with $z \leq 0.03$ and $B \leq 14.5$ taken from the catalogue of Lipovetsky *et al.* (1987). In addition, we included in our sample the following objects: Seyferts linear radio sources and barred Seyferts with known [OIII] emission–line images and [OIII] emission–line profiles.

Table 1. Journal of observations

Name	*Other*	*Sy*	*RC3 type*	*Date*	*Filter*	*Exposure*	*Seeing*
Mkn 3	UGC 3426	2.0	S0:	06/07.12.94.	V	3 x 600	1.3
Mkn 3				06/07.12.94.	I	3 x 600	2.4
Mkn 530	NGC 7603	1.0	SA(rs)b: pec	07/08.12.94.	V	3 x 600	1.7
Mkn 530				07/08.12.94.	I	3 x 600	1.5
Mkn 533	NGC 7674	2.0	SA(r)bc pec	04/05.09.94.	V	3 x 600	1.5
Mkn 533				22/23.07.93.	R	2 x 600	1.8
Mkn 573	UGC 1214	2.0	(R)SAB(rs)0+:	04/05.09.94.	V	2 x 600	1.6
Mkn 573				04/05.09.94.	I	2 x 600	1.4
Mkn 744	NGC 3786	1.8	SAB(rs)a pec	09/10.02.94.	V	2 x 600	3.0
Mkn 744				09/10.02.94.	R	2 x 600	2.7
Mkn 955	MCG 0-2-94	2.0	S?	05/06.09.94.	V	3 x 600	1.3
Mkn 955				05/06.09.94.	I	3 x 600	1.9
Mkn 1058		2.0	S?	05/06.09.94.	V	3 x 600	2.0
Mkn 1058				05/06.09.94.	I	3 x 600	2.3
Mkn 1066	UGC 2456	2.0	(R)SB(s)0+	03/04.09.94.	V	3 x 600	2.3
Mkn 1066				03/04.09.94.	I	3 x 600	2.4
Mkn 1073	UGC 2608	2.0	(R′)SB(s)b	06/07.12.94.	V	3 x 600	1.5
Mkn 1073				06/07.12.94.	I	3 x 600	1.5
Mkn 1157	NGC 591	2.0	(R′)SB0	10/11.12.94.	V	3 x 600	1.7
Mkn 1157				10/11.12.94.	I	3 x 600	1.7
NGC 1019	UGC 2131	1.0	SB(rs)bc	28/29.09.95.	V	3 x 600	2.7
NGC 1019				28/29.09.95.	R	3 x 600	2.7
NGC 3185	UGC 5554	1.0	(R)SB(r)a	26/27.12.94.	V	3 x 600	2.0
NGC 3185				26/27.12.94.	I	3 x 600	2.0
UGC 524	MCG 5-3-13	1.0	(R′)SB(s)b	06/07.12.94.	V	3 x 600	2.0
UGC 524				06/07.12.94.	I	4 x 600	1.6
UGC 3223	MCG 1-13-12	1.0	SBa	07/08.12.94.	V	3 x 600	1.6
UGC 3223				07/08.12.94.	I	3 x 600	3.0
UGC 3995	MCG 5-19-1	2.0	S pec	05/06.12.94.	V	3 x 600	2.7
UGC 3995				05/06.12.94.	I	3 x 600	2.4

In this paper we present the first results of our survey. The observation and data reduction techniques are described in Section 2. A brief description of the morphology for individual objects as well as results of the ellipse–fitting analysis are presented in Section 3. A summary is provided in Section 4.

2 OBSERVATIONS AND DATA REDUCTION

The observations were carried out with the 1 m telescope at the Special Astrophysical Observatory of the Russian Academy of Sciences. The images were obtained using the 530×580 CCD camera with a pixel size of 18×24 microns ($0.29'' \times 0.38''$), a gain of 3.7 electron/ADU and readout noise 20–23 electrons (Afanasiev *et al.*, 1991a–f). Details of the observations are given in Table 1.

The images were reduced using the following procedures:

(1) subtraction of the bias frame;

(2) flat–field correction;

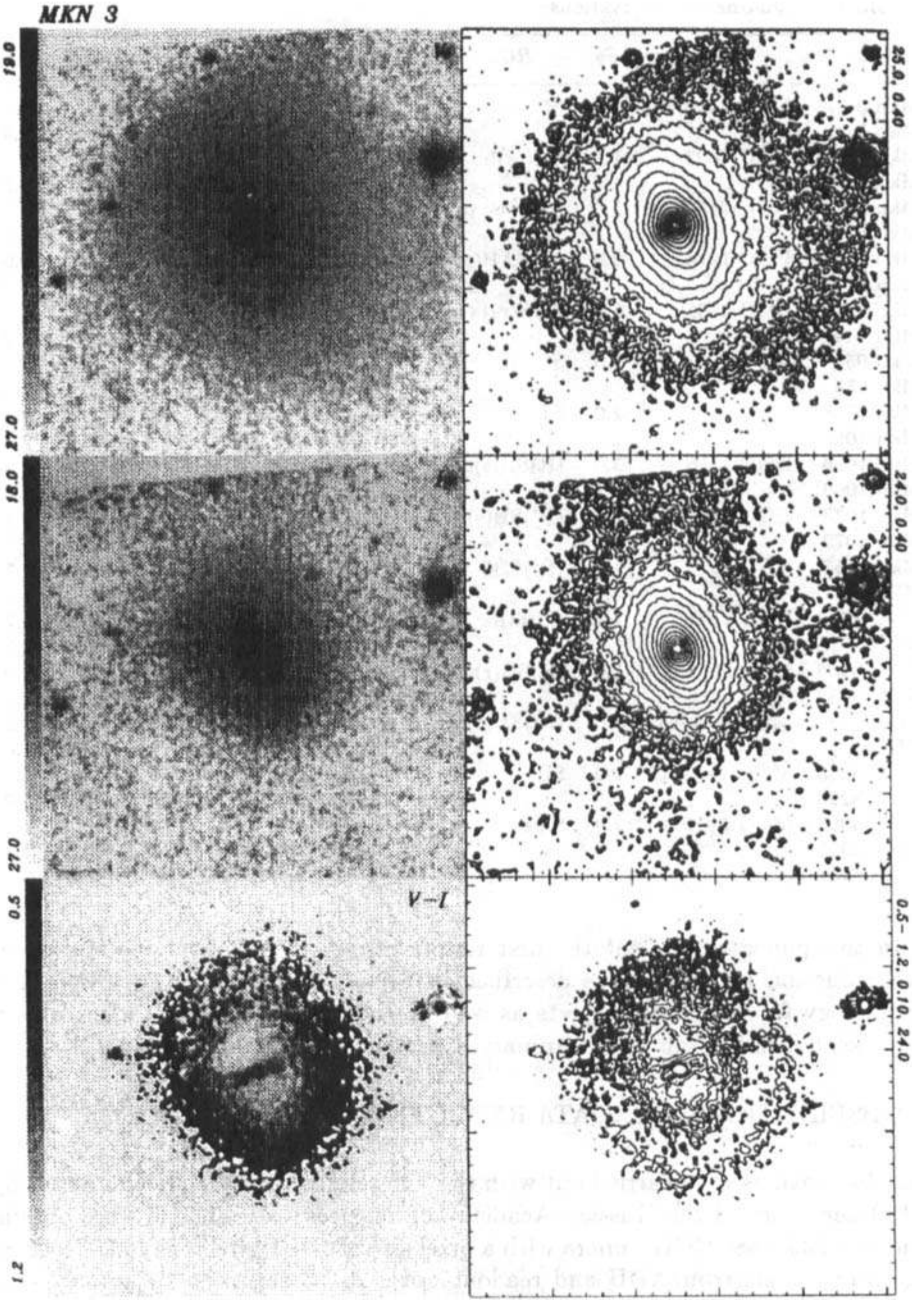

Figure 1 Grey-scale and contour maps for direct images and colours of each galaxy in this paper. The north is to the top and east is to the left. The field of view is 113 × 113 arcseconds and one scale graduation equals 4.4 arcseconds. The values near each isophote map give the outer contour level and the step. Those near each colour contour plot are the colour interval, the step and the outer contour level for the colour representation.

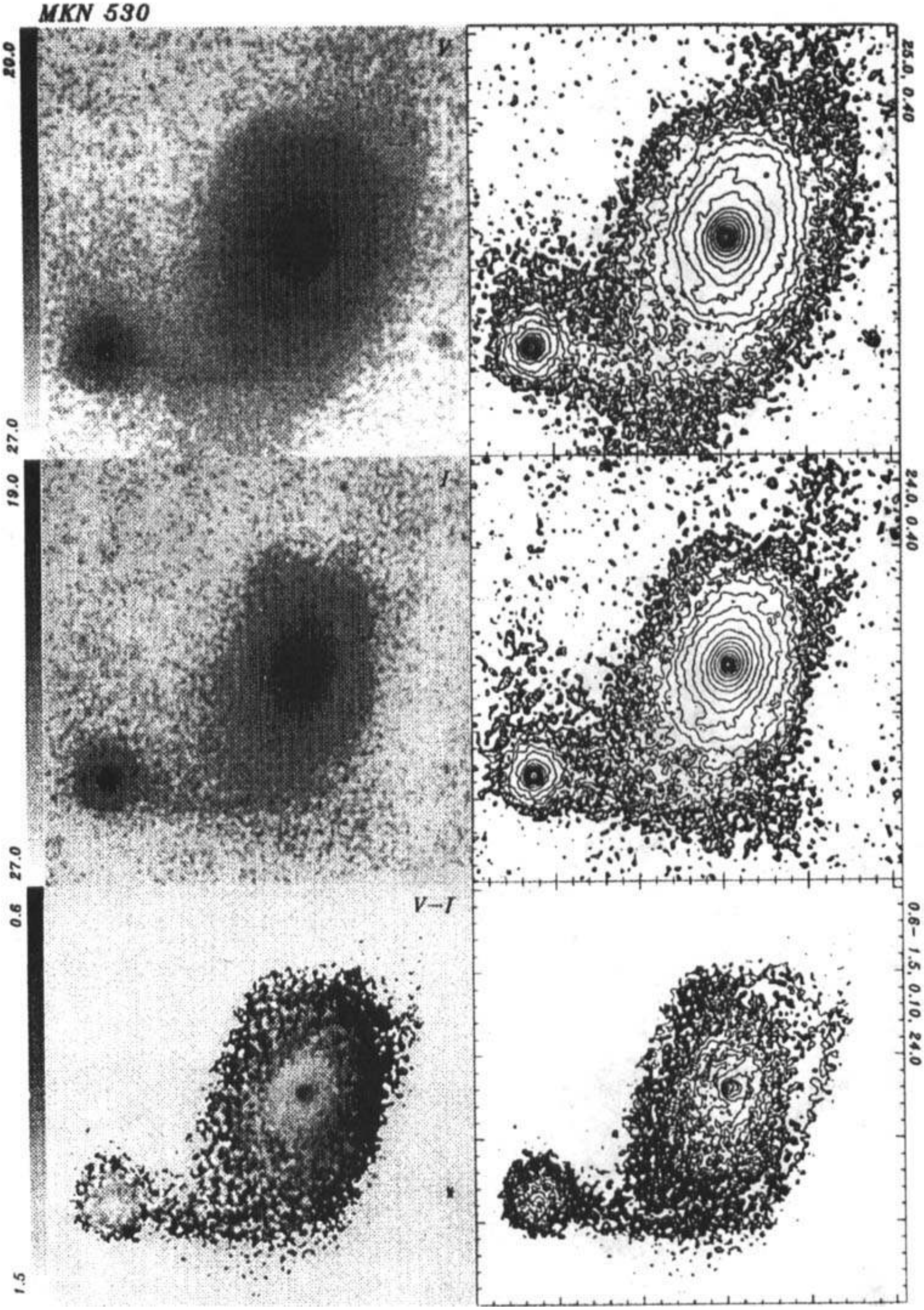

Figure 1 Continued.

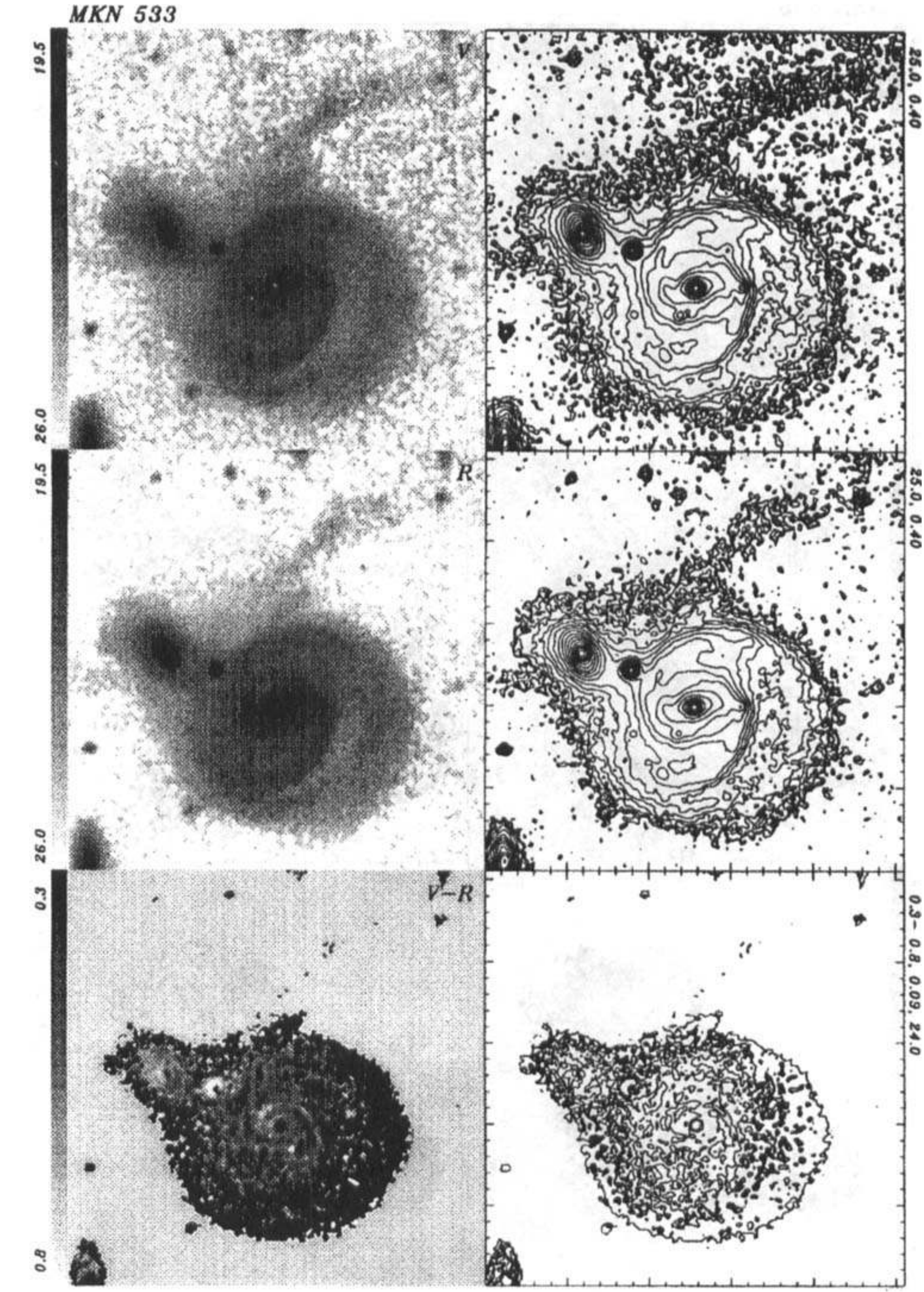

Figure 1 Continued.

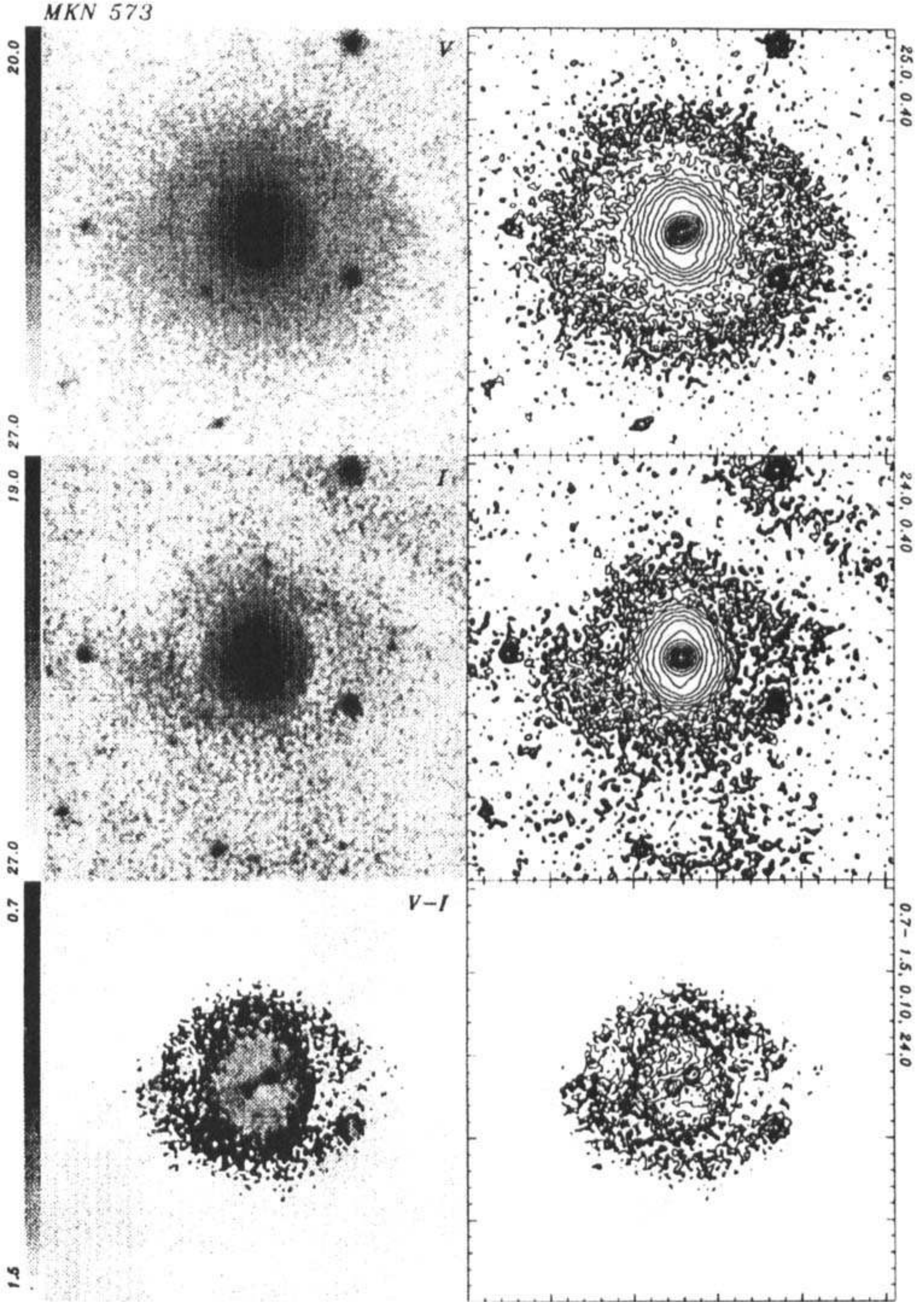

Figure 1 Continued.

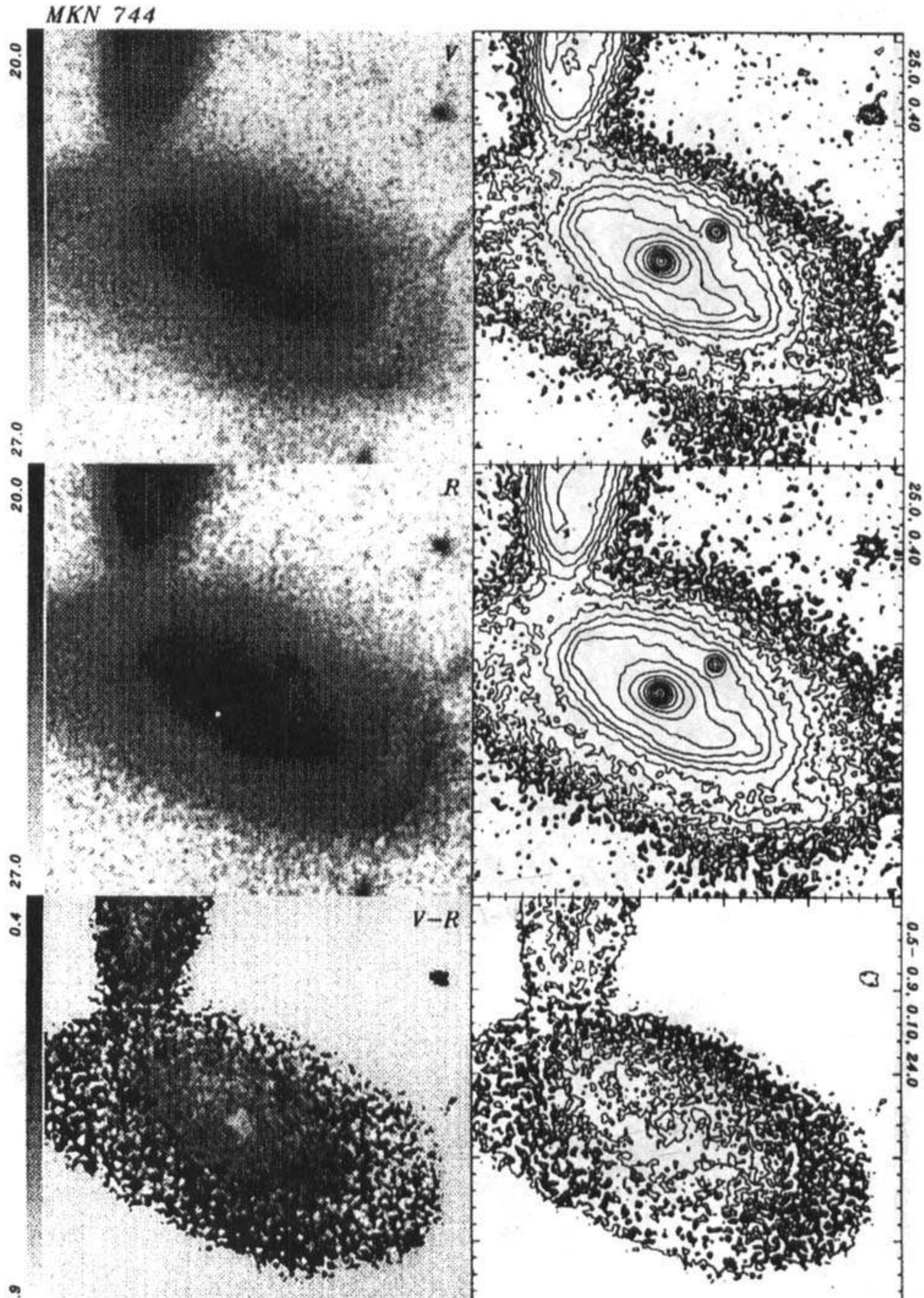

Figure 1 Continued.

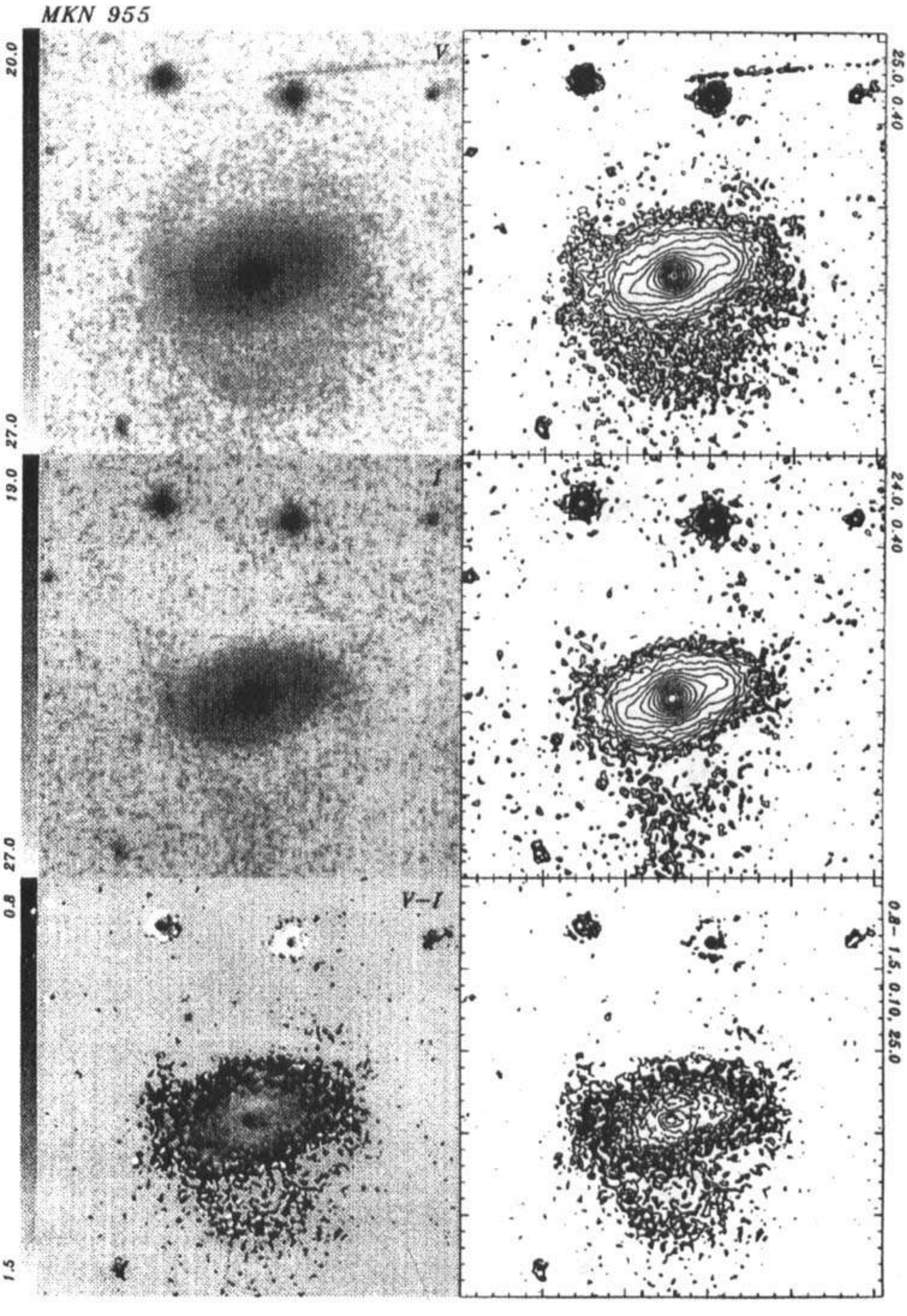

Figure 1 Continued.

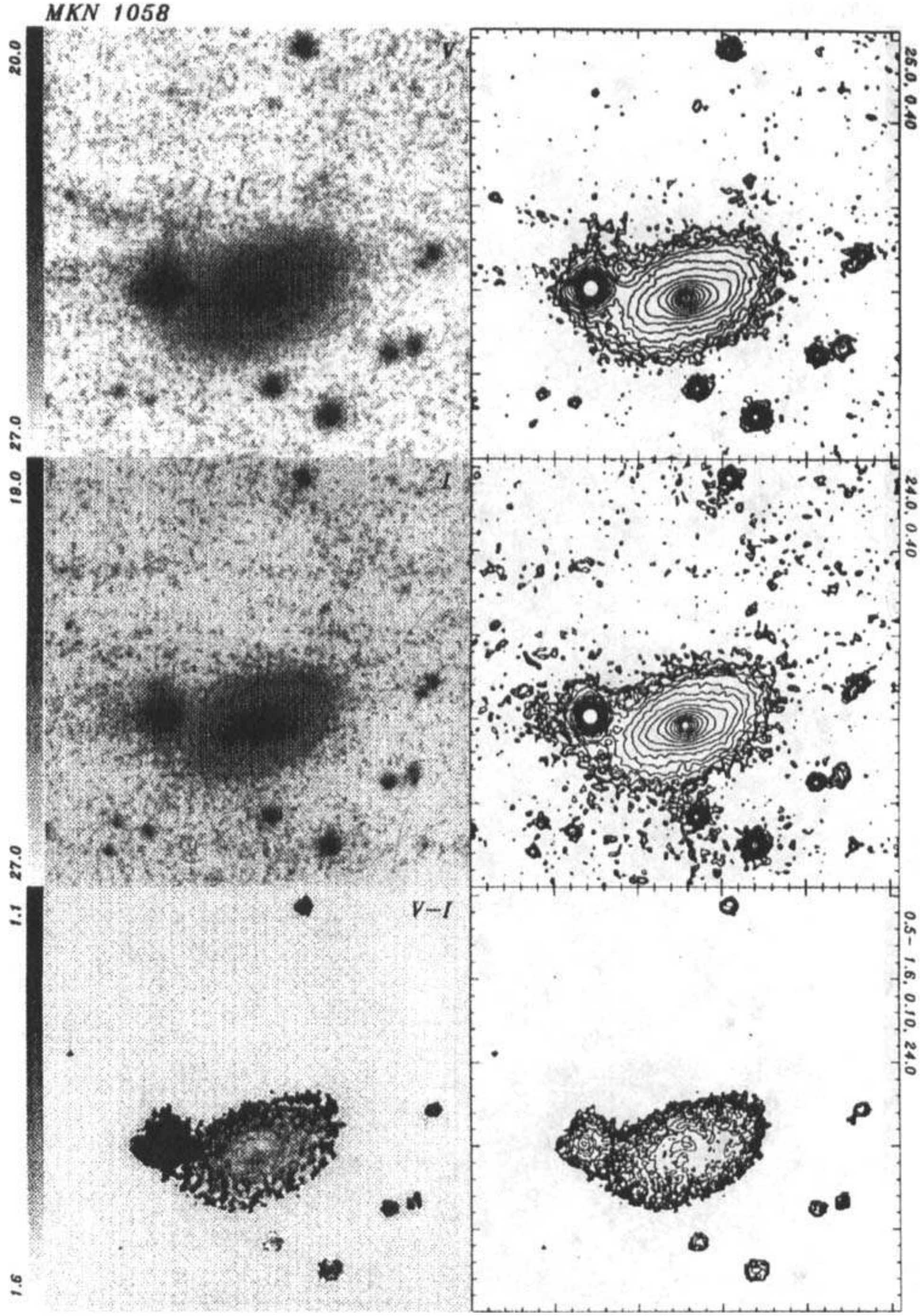

Figure 1 Continued.

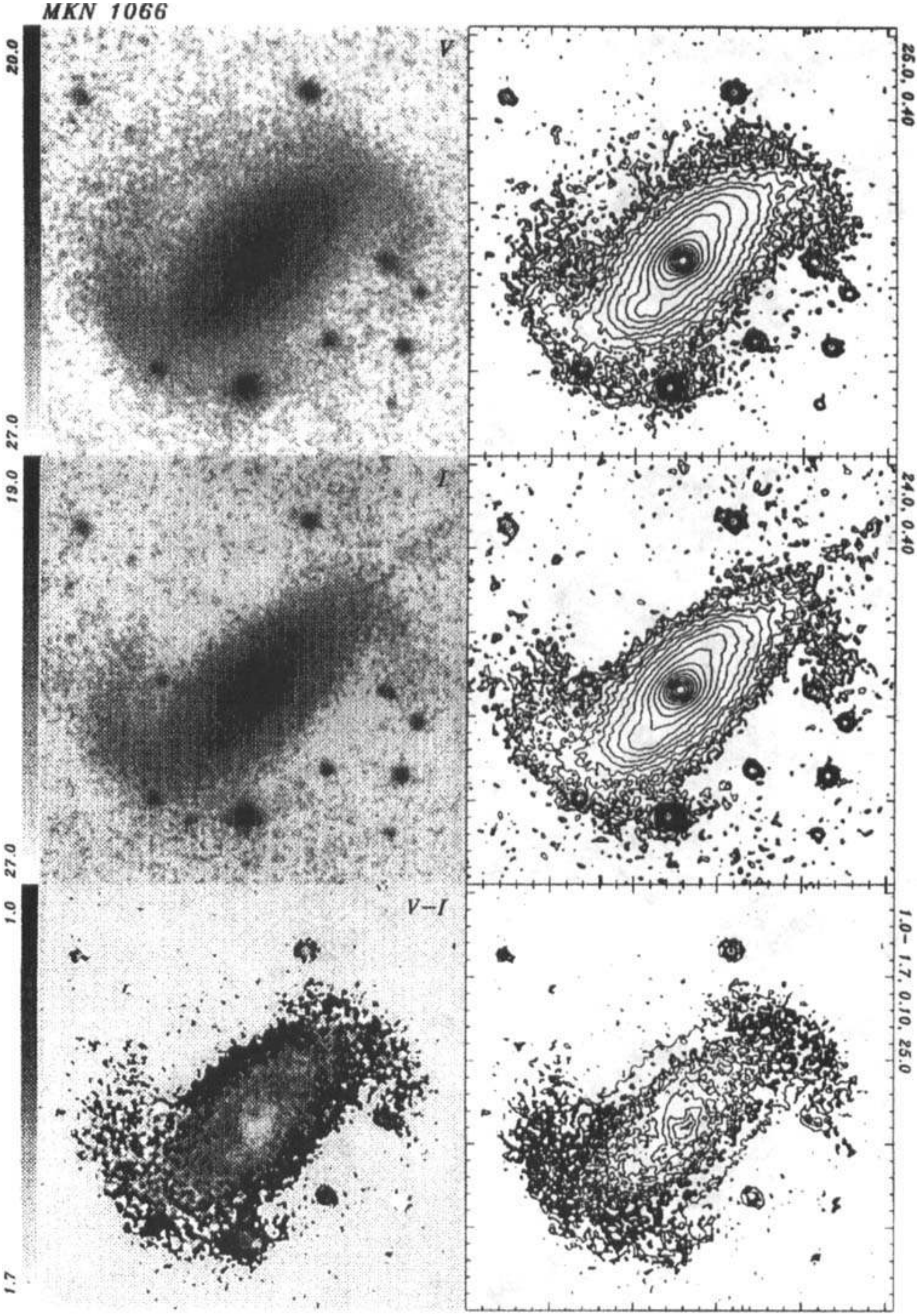

Figure 1 Continued.

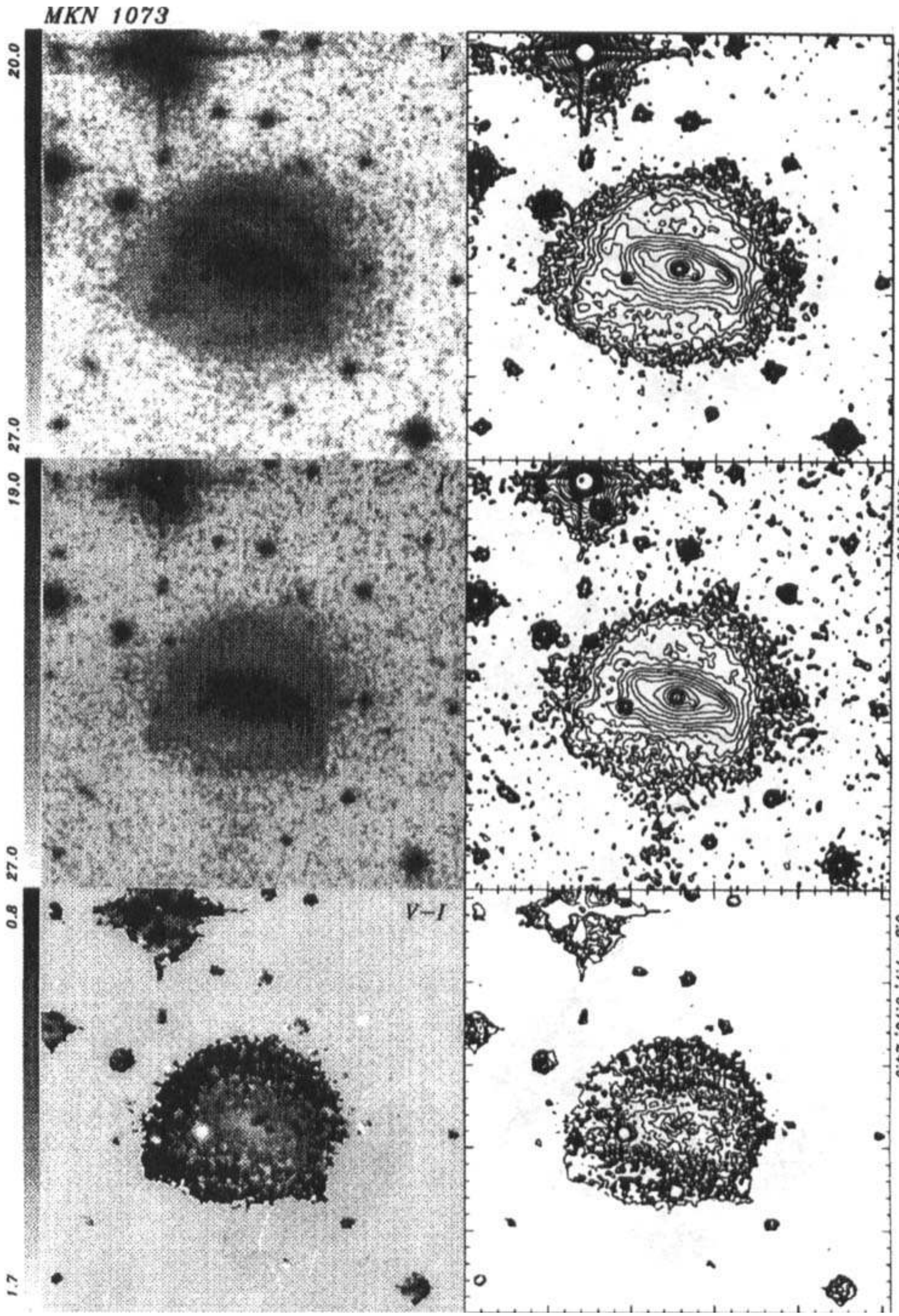

Figure 1 Continued.

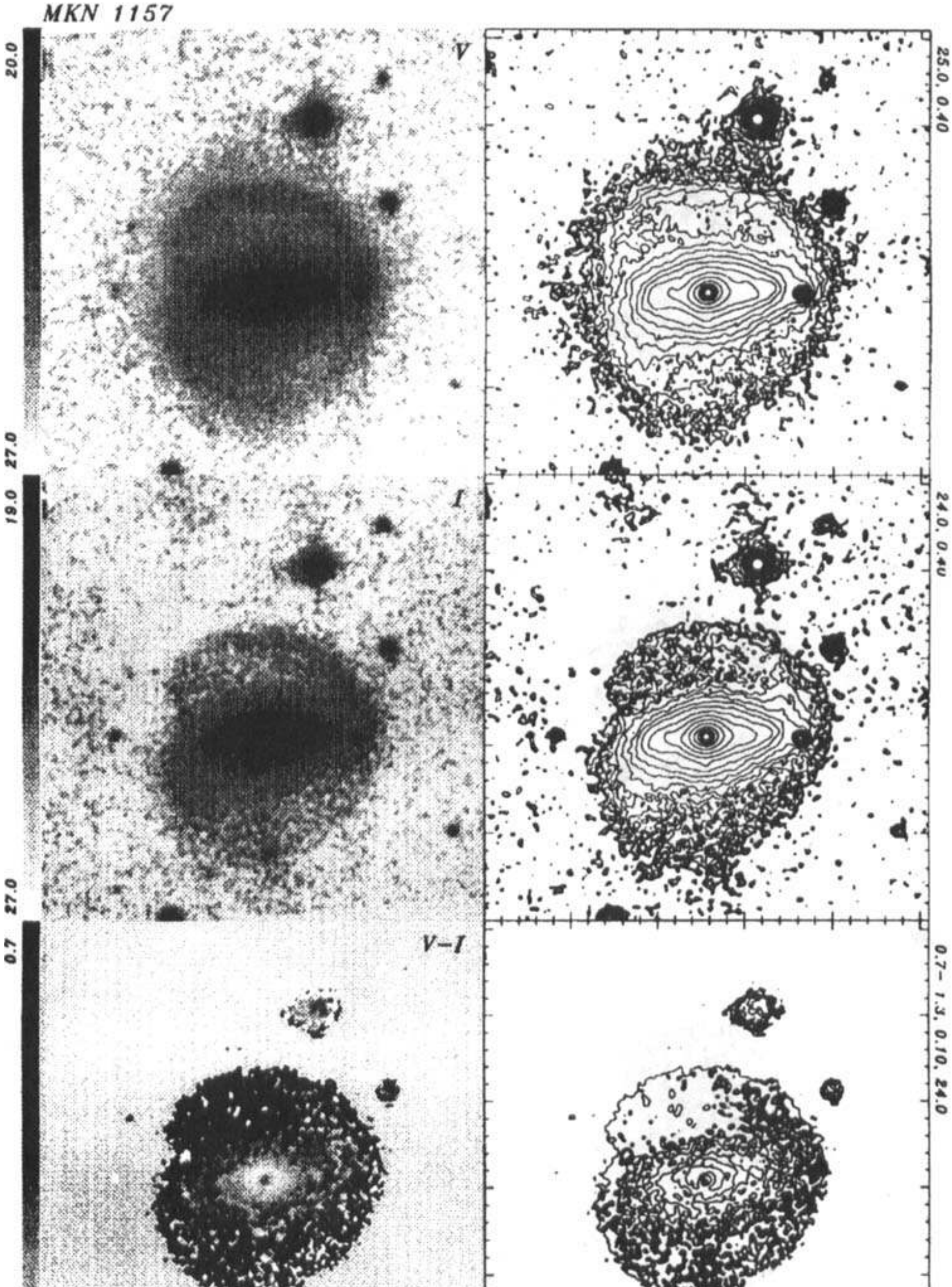

Figure 1 Continued.

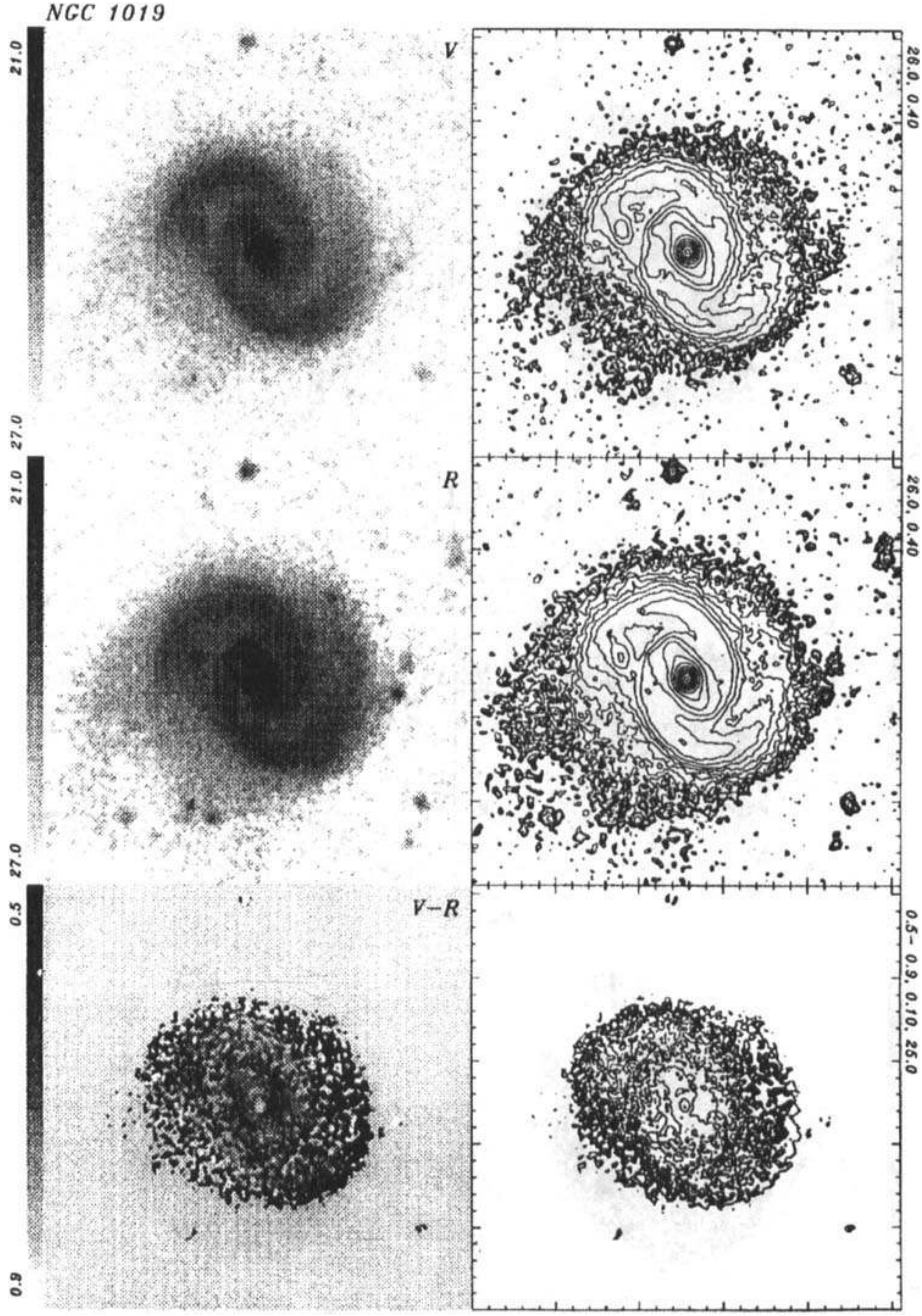

Figure 1 Continued.

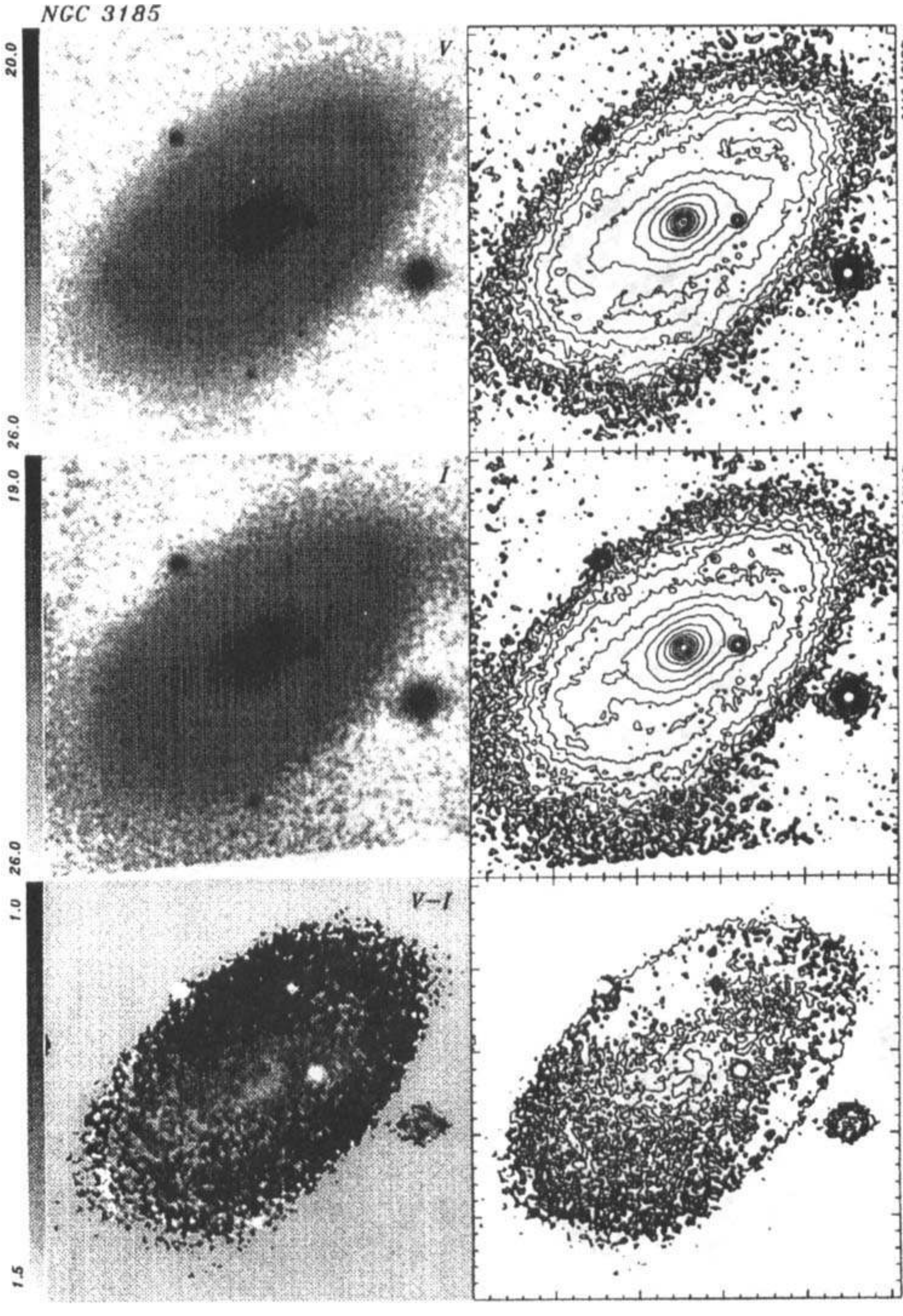

Figure 1 Continued.

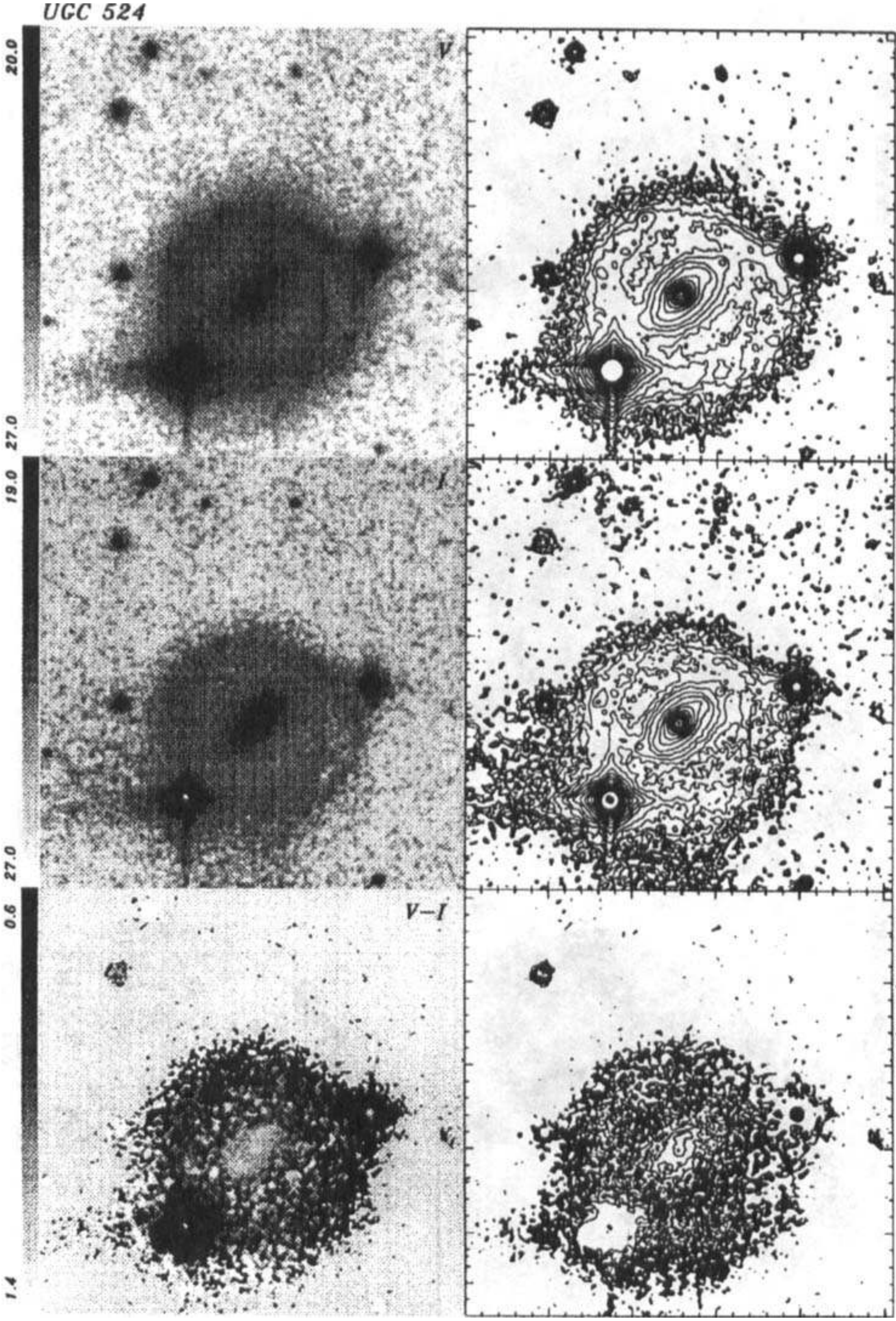

Figure 1 Continued.

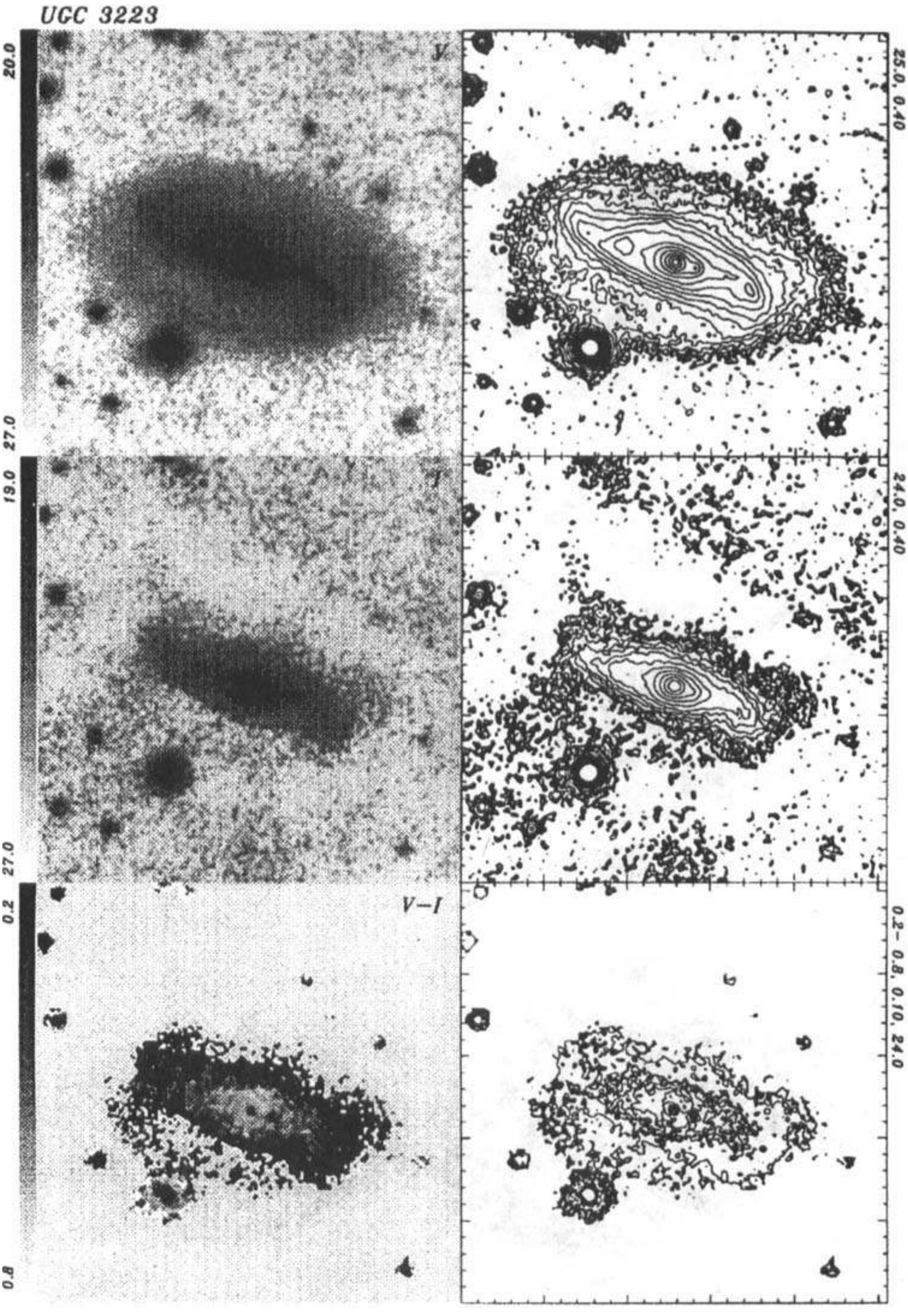

Figure 1 Continued.

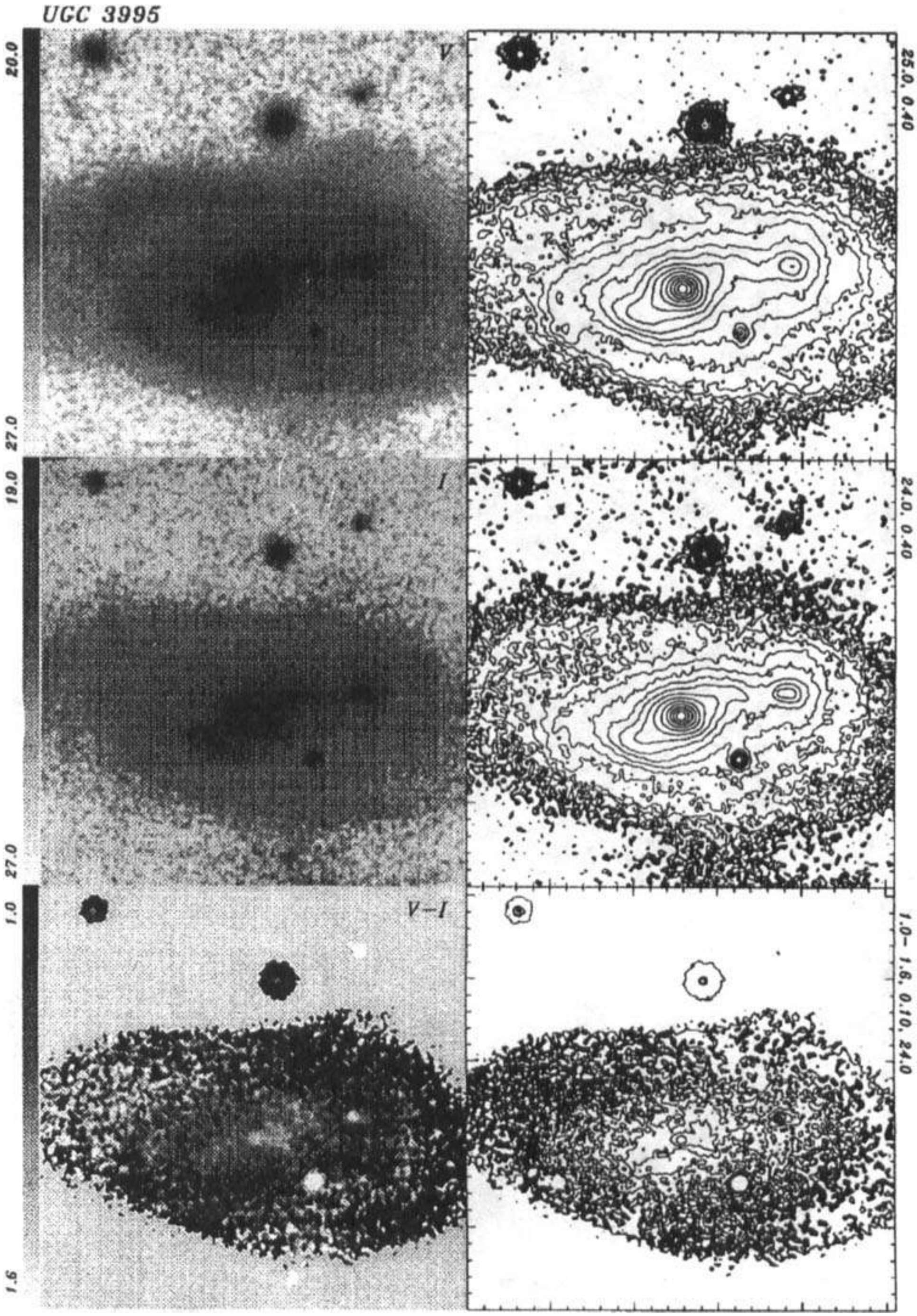

Figure 1 Continued.

(3) removal of cosmic ray hits and correction of values in bad pixels;

(4) scale transformation;

(5) sky background subtraction.

The source frames were bias–subtracted. Generally several bias frames were taken during each night and median–combined to obtain an averaged bias frame. Variations in sensitivity across the CCD from pixel to pixel were corrected with a flat–field frame. The flat–field frame was obtained as the mean of the number of dusk sky exposures each night. In order to remove cosmic ray hits and correct values in bad pixels we made two or three exposures for each galaxy with a small shift along CCD rows. Corrected frames were then coadded and the scale was changed to transform the pixel shape to a square shape. The result scale is 0.44″ per pixel, thus one graduation in Figure 1 equals 4.4″. Finally the frames were median smoothed with 3×3 pixel window in order to improve the signal–to–noise ratio.

To determine the sky background the galaxy and field stars were masked. The sky frame was calculated then as a polynomial leastsquares fit.

In order to calibrate our images, we observed a number of fields with standard stars (Christian *et al.*, 1985; Landolt, 1992). During each night 2–5 measurements of standard sequences were made with three filters. The transformation to the standard system was made by using the following equations:

$$
\begin{aligned}
V &= v + 21.092 - 0.234X - 0.077(v - r) \\
V &= v + 21.011 - 0.221X - 0.040(v - i) \\
R &= r + 21.343 - 0.232X + 0.002(v - r) \\
I &= i + 19.898 - 0.076X - 0.003(v - i)
\end{aligned}
$$

where X is the air mass; v, r, i are the instrumental magnitudes and V (Johnson), R, I (Cousins) are standard magnidutes. The zero points are calculated for a one–second exposure.

Corrected in this way the images were then analysed by fitting ellipses to the isophotes in the two bands. This technique allowed us to identify embedded structures (such as bars) and gives structural parameters of these structures (such as orientation and ellipticity). The algorithm used in the ellipse–fitting program is described in details in Bender and Möllenhoff (1987).

3 NOTES ON INDIVIDUAL OBJECTS

In this section we provide a brief description of the main features observed for each galaxy. As a general rule, the parameters measured in the V band are given in the text. The position angles and the axial ratios of the bars and the outer isophotes for the VI(R) bands are presented in Table 2. Figure 1 displays the images, the colour and contour maps for each galaxy in this paper. The results of elliptical fits are provided in Figure 2 as surface brightness, position angle and ellipticity profiles.

Table 2. Parameters of the bars and the outer isophotes for the V and $I(R)$ band

	Bar					Outer isophote			
	V			$I(r)$		V		$I(R)$	
Name	*a*	*b/a*	*PA*	*b/a*	*PA*	*b/a*	*PA*	*b/a*	*PA*
(1)	*(2)*	*(3)*	*(4)*	*(5)*	*(6)*	*(7)*	*(8)*	*(9)*	*(10)*
Mkn 3	15.0	0.68	23	0.66	23	0.92	57	...	...
Mkn 530	6.0	0.81	163	0.80	164	0.58	152	0.60	158
Mkn 533	8.0	0.48	107	0.49	106	0.90	88	0.90	74
Mkn 573(p)	9.0	0.70	174	0.68	179	0.87	90	0.75	158
Mkn 573(s)	2.6	0.71	112	0.90	96	...	...	...	...
Mkn 744(p)	25.0	0.38	58	0.40	58	0.51	67	0.49	68
Mkn 744(s)	7.0	0.71	75	0.72	73	...	...	...	...
Mkn 955	15.5	0.38	110	0.41	109	0.91	157	0.55	103
Mkn 1058	12.0	0.47	103	0.47	104	0.63	119	0.58	115
Mkn 1066(p)	15.5	0.39	142	0.42	143	0.79	125	0.42	126
Mkn 1066(s)	2.5	0.81	113	0.81	112	...	...	...	...
Mkn 1073	11.7	0.33	80	0.36	79	0.77	91	0.80	95
Mkn 1157	14.8	0.37	94	0.39	94	0.95	170	0.87	151
NGC 1019	9.8	0.51	30	0.48	28	0.87	77	0.88	94
NGC 3185(p)	30.0	0.43	113	0.36	113	0.59	131	0.56	132
NGC 3185(s)	2.3	0.79	134	0.80	133	...	...	...	...
UGC 524	8.6	0.52	139	0.52	138	0.93	139	0.95	-10
UGC 3223	5.3	0.51	72	0.60	73	0.55	78	0.38	73
UGC 3995	15.2	0.49	116	0.46	116	0.55	85	0.56	88

Note. Col.(*1*), Object name; col.(*2*), semi-major axis of the bar (in arcseconds) defined at maximum ellipticity; col.(*3–6*), axial-ratio and position angle (in degrees) of the bar defined at maximum ellipticity for the V and I/R band; col.(*7–10*), axial-ratio and position angle (in degrees) of the outer isophote for the V and $I(R)$ band. Comments: (p), primary bar; (s), secondary bar.

3.1 Mkn 3

This galaxy has been previously classified as uncertain S0: in RC3 and SB0 by Shuder and Osterbrock (1981). Our images in both the V and I bands show the large-scale bar which is revealed as the maximum in the ellipticity curve at the $15''$ distance with $e = 0.32$ and PA = 23°. At the $4''$ distance the V isophote map reveals a perturbation with PA = 112° which is perpendicular to the bar and clearly seen in the V band only. In the innermost region the position angle curve shows a sharp change from PA = 23° to PA = 81° at the $1.5''$ radius. The I distribution shows no sign of a similar feature on the same scale.

The $V - I$ colour map shows a curved jet-like structure in the inner region. The position angle of the colour contours rotates from PA = 90° to PA = 111° at distances $2''$ and $4''$, respectively. These colour features correspond to those in the direct V image. The innermost structure is aligned with the [OIII] major axis at PA = 82° on the 1–3 scale (Haniff *et al.*, 1988; Capetti *et al.*, 1995) as well as with the double radio axis at PA = 85° (Wilson *et al.*, 1980; Ulvestad and Wilson,

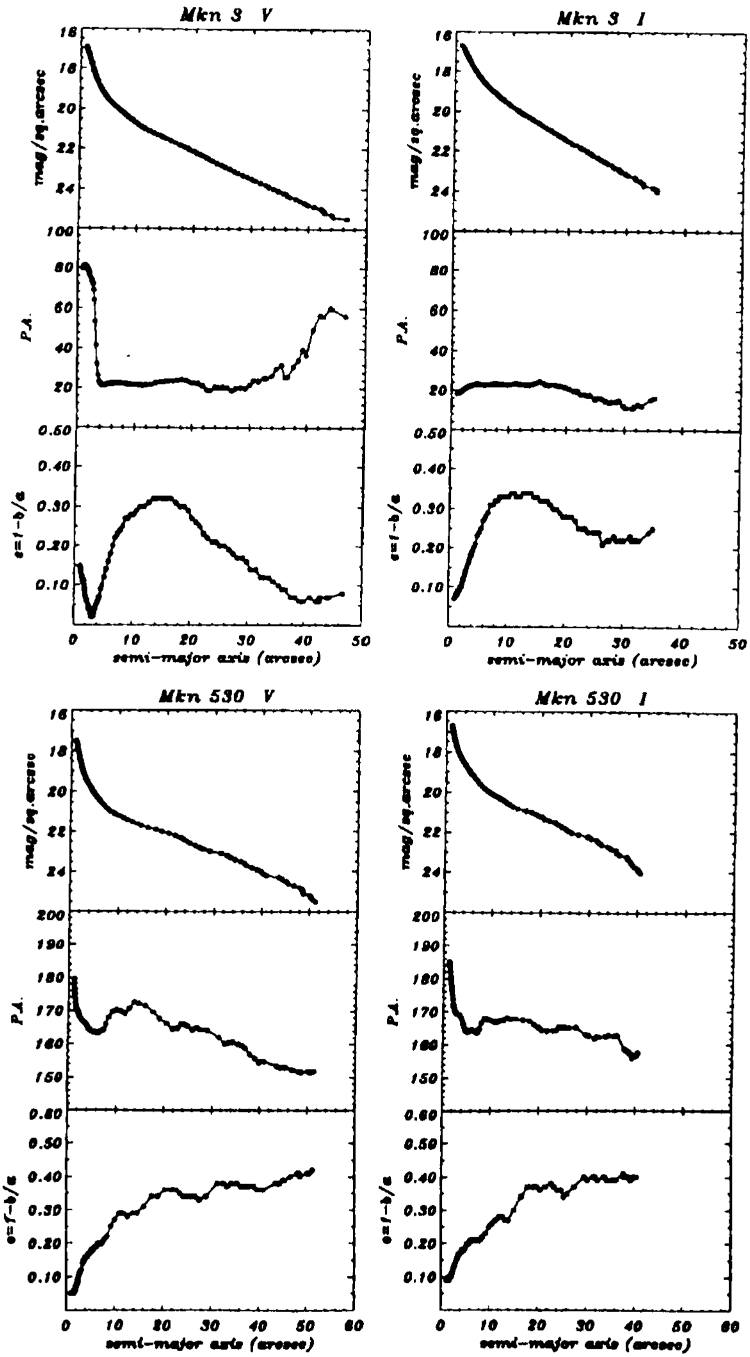

Figure 2 Results of elliptical fits to isophotes for each galaxy in this paper: (from top to bottom in each of the panels) surface brightness, major-axis position angle (in degrees) and ellipticity profiles as a function of projected semi-major axis.

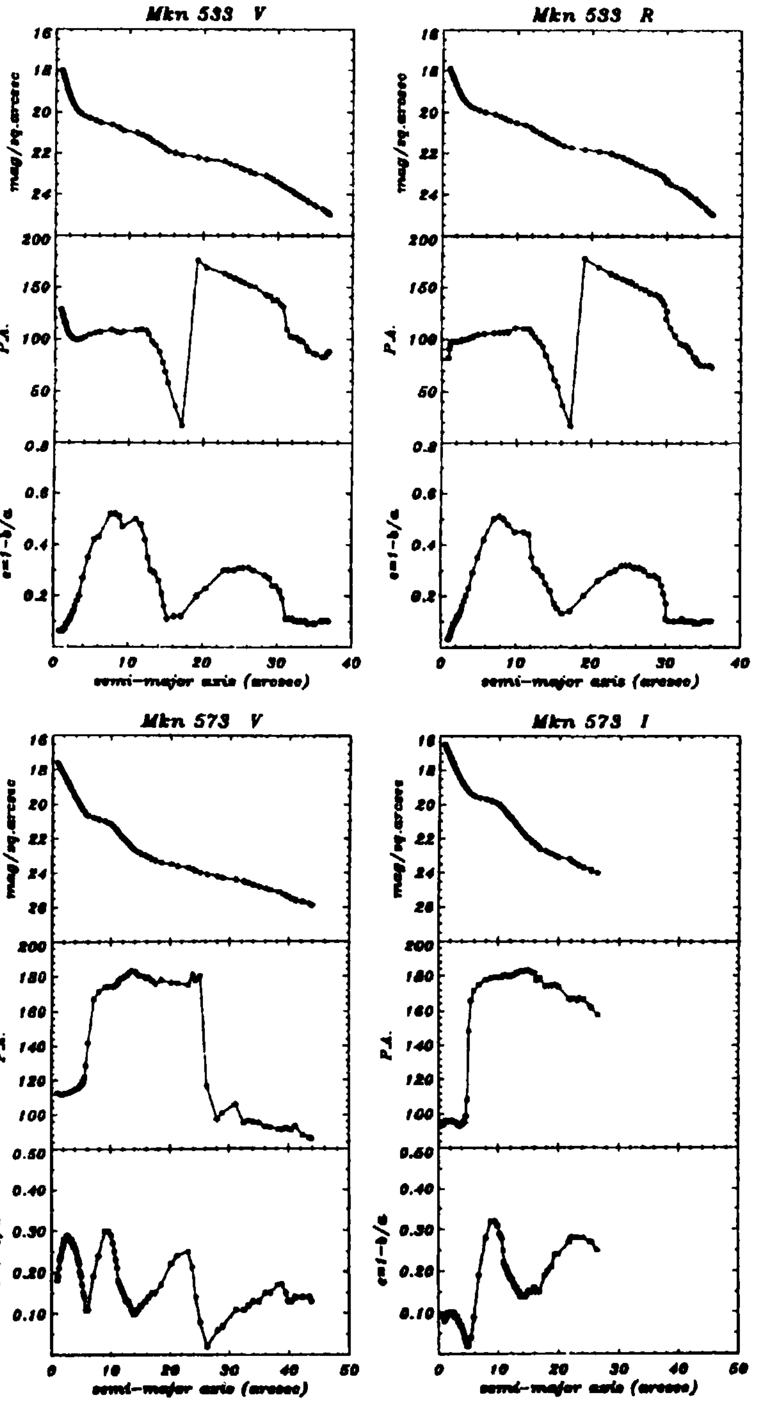

Figure 2 Continued.

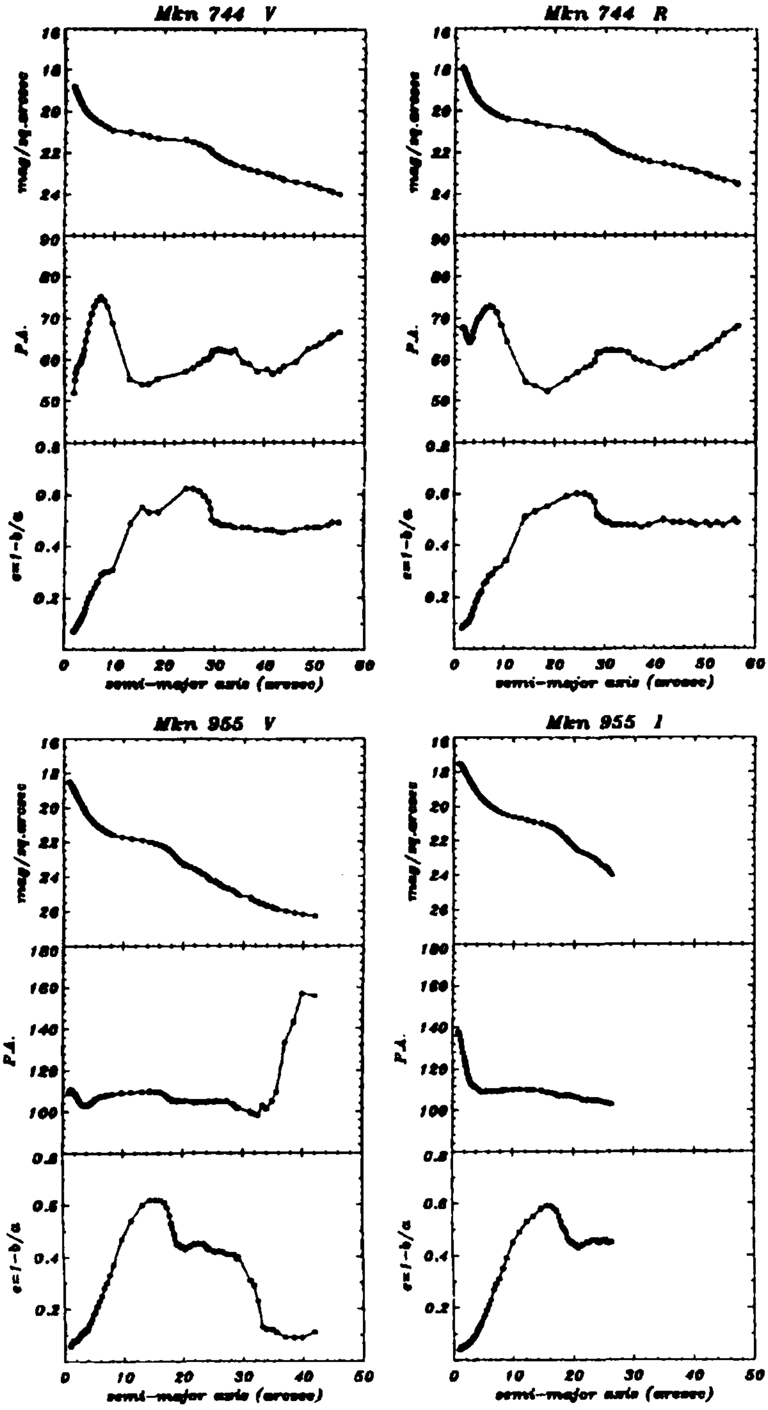

Figure 2 Continued.

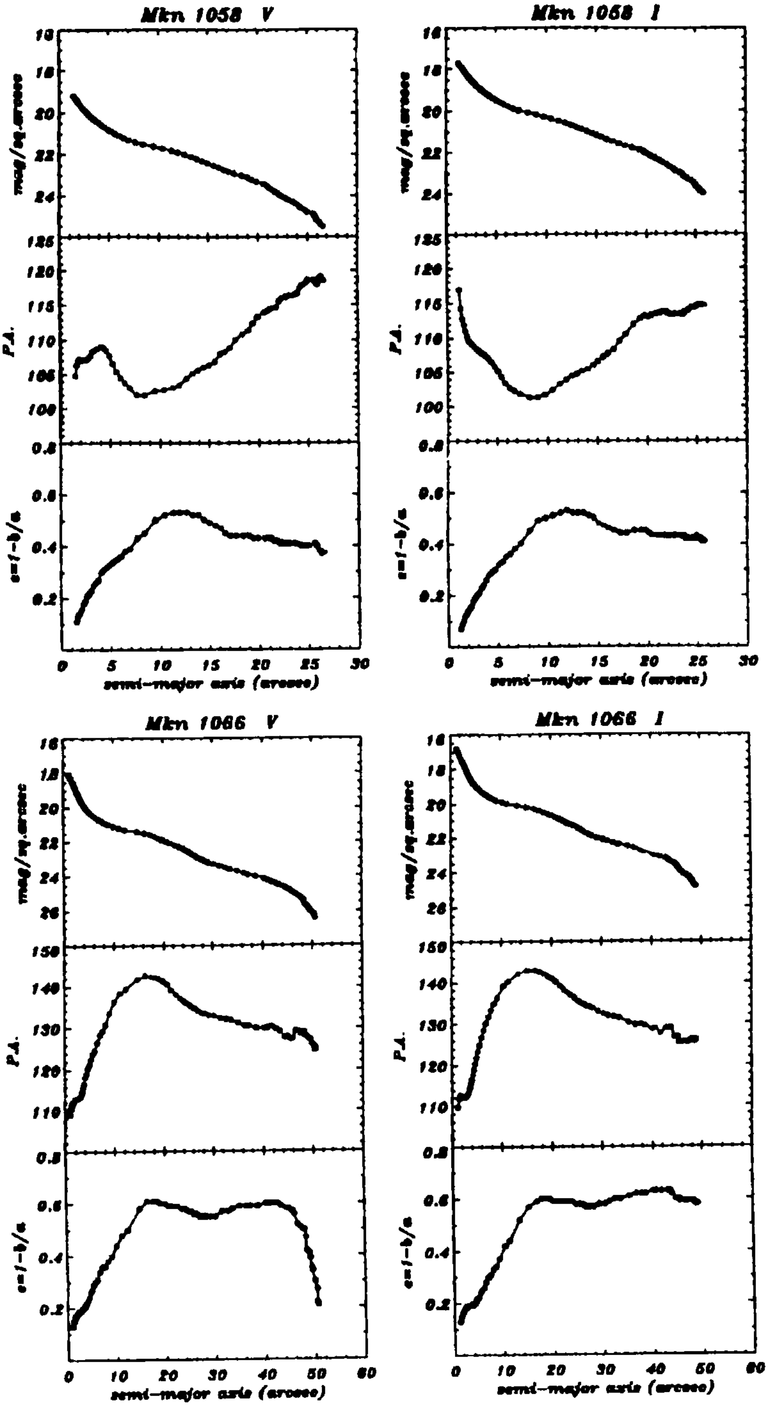

Figure 2 Continued.

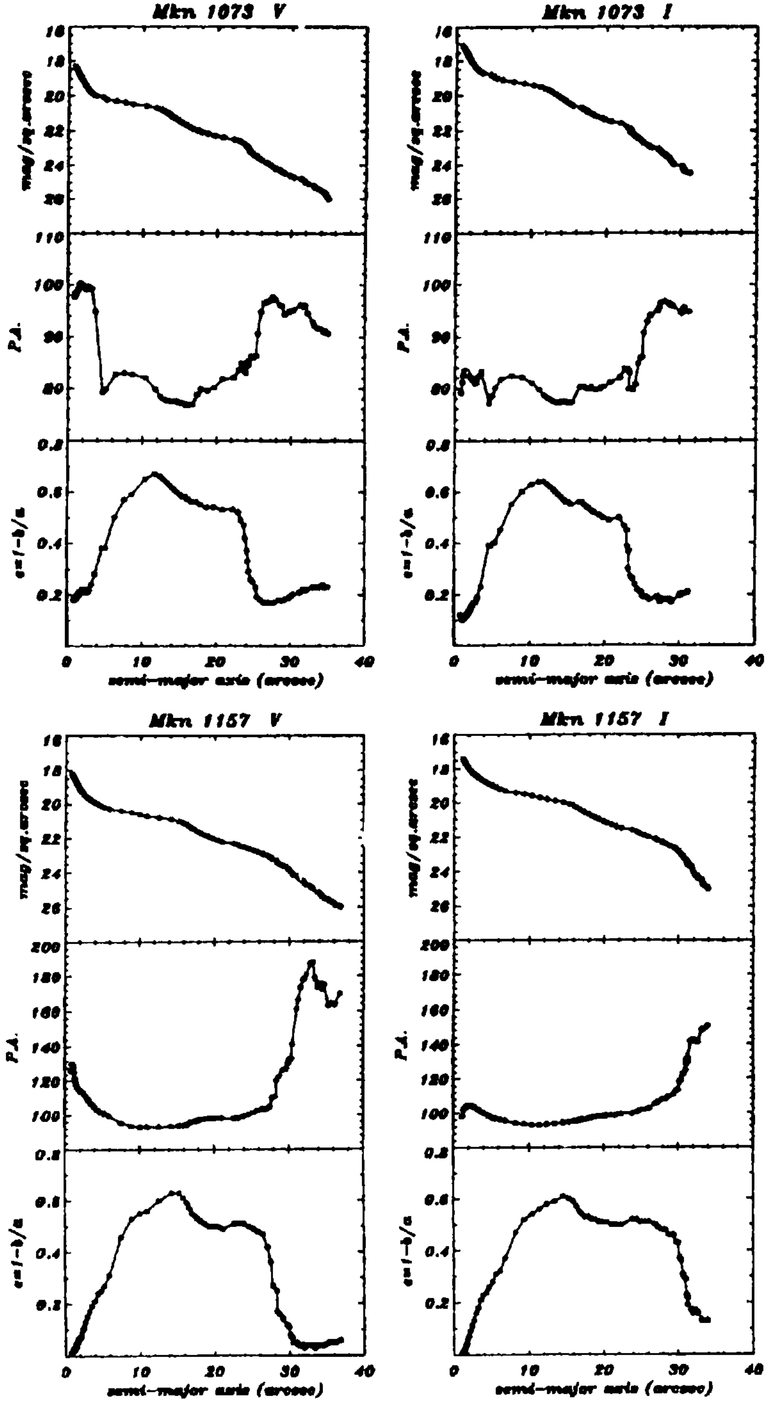

Figure 2 Continued.

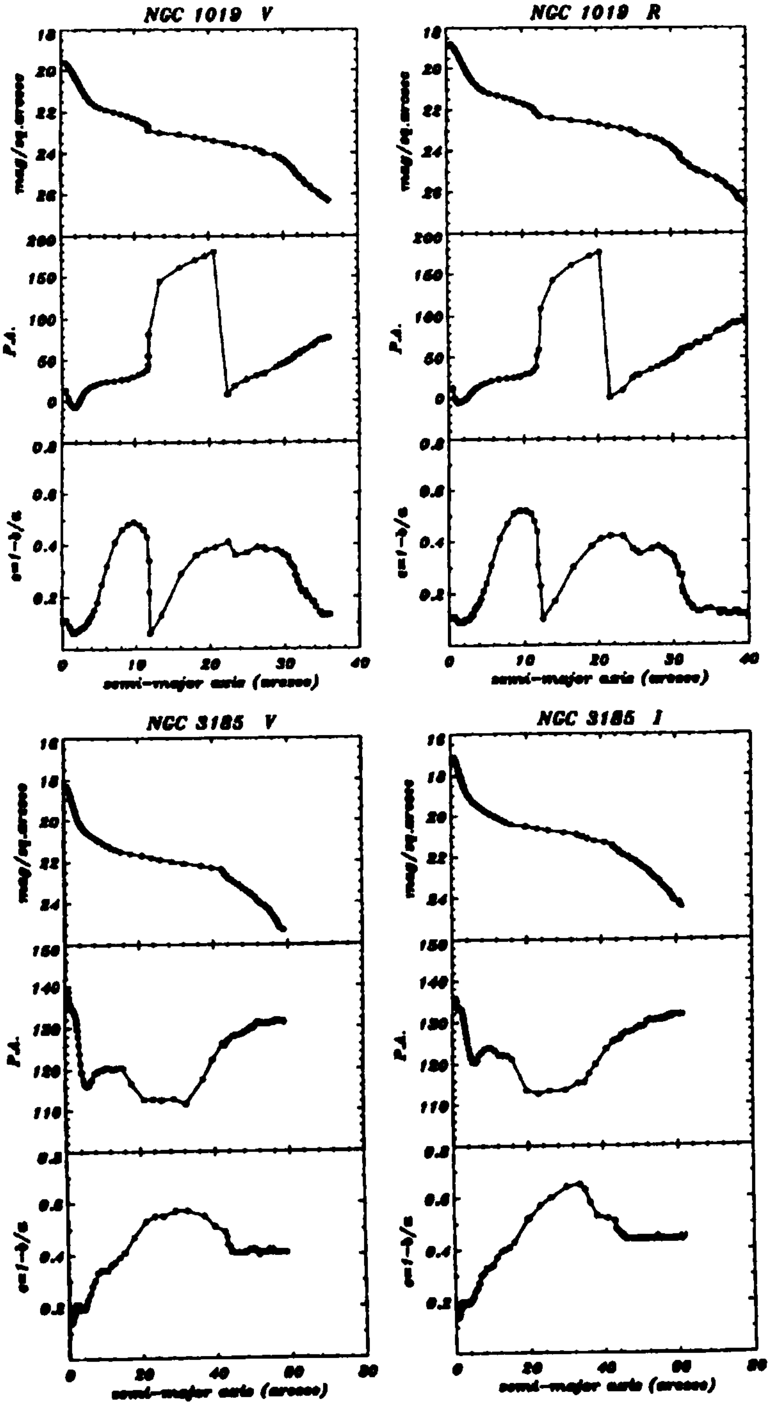

Figure 2 Continued.

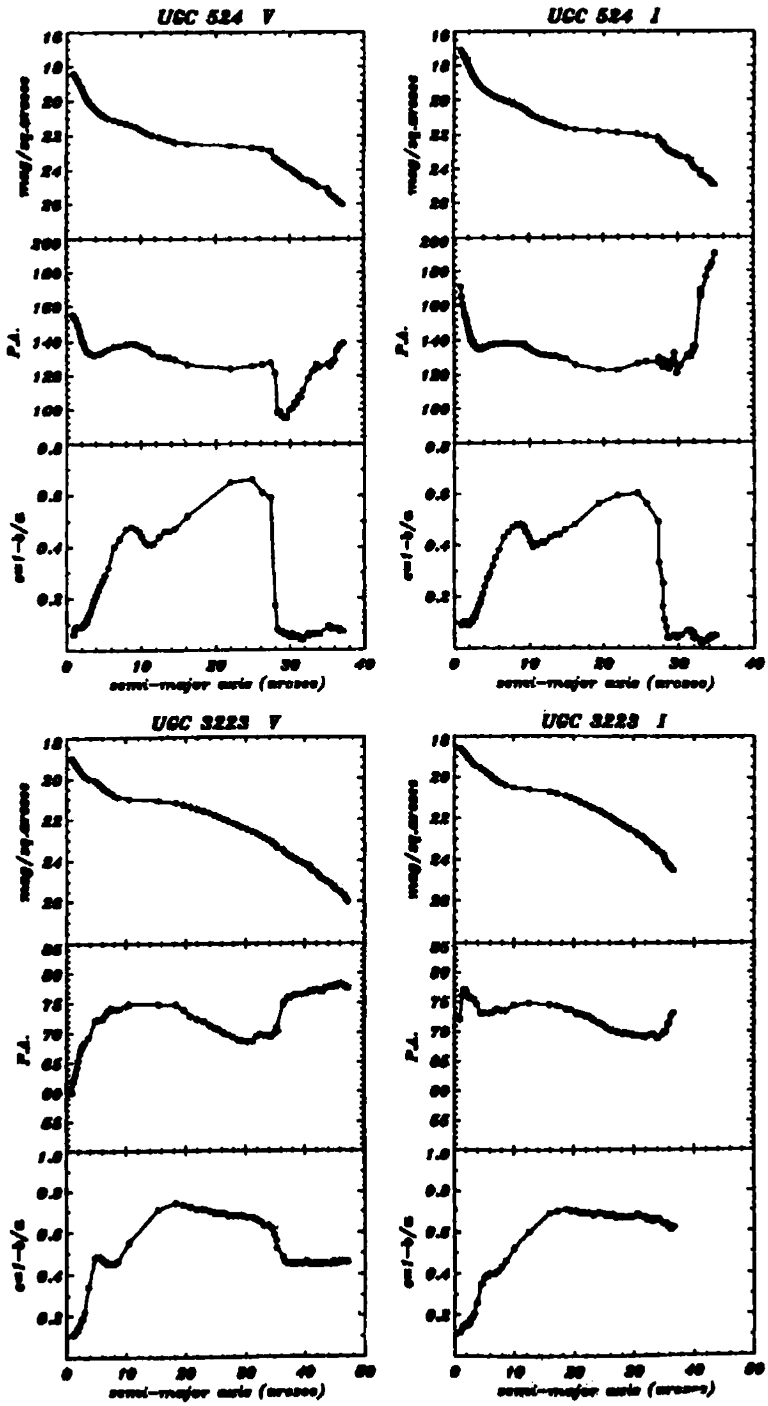

Figure 2 Continued.

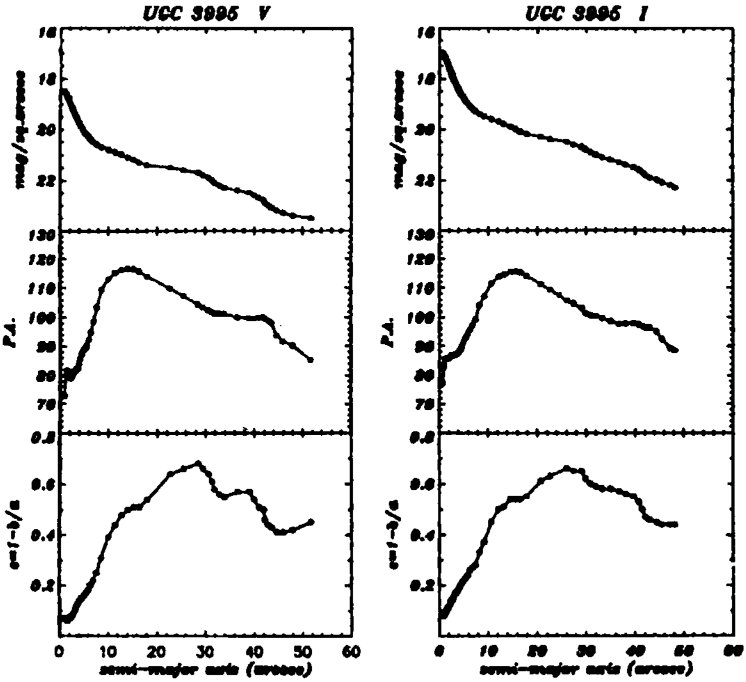

Figure 2 Continued.

1984). The colour feature at the 4″ distance is very similar to the [OIII] biconical structure at PA = 114° on the same scale (Pogge and De Robertis, 1993).

3.2 Mkn 530 = NGC 7603

This galaxy has been previously classified as SA(rs)b:pec in RC3. Our V and I images possibly show an inner ring-like structure at distance 20″ from the centre. A similar feature was discussed previously by Arp (1971) and more recently by Sharp (1986). In the V band the position angle curve shows a local minimum at the 6″ radius (PA = 163°) compared with the 14″ radius (PA = 173°). The same is seen in the I band, which makes it possible to suppose the presence of a bar-like structure on this scale.

3.3 Mkn 533 = NGC 7674

This galaxy has been previously classified as SA(r) bc pec in RC3 but we did not find hints of an inner ring structure. The maximum in the ellipticity curve at the 8″ distance indicates the presence of a bar with e = 0.52 and PA = 107°. The radio map shows a double source with major axis at PA = 113° (Unger *et al.*, 1986) which is aligned with the bar direction.

The presence of the bar in this galaxy was discussed previously by McLeod and Rieke (1995) and Afanasiev and Kostiuk (1996).

3.4 Mkn 573

This galaxy is a clear example of a double-barred system. Two maxima in the ellipticity curve correspond to plateaux in the position angle profile in both the V and I bands. The primary bar is revealed as the maximum in the ellipticity curve at the $9''$ distance with $e = 0.30$ and PA = 174°. Another maximum at the $2.6''$ distance indicates the presence of a secondary bar with $e = 0.29$ and PA = 112°. However, in the I band the secondary maximum is fainter than the primary one and thus the bar is less elliptical ($e = 0.10$, PA = 96°) for the secondary, and $e = 0.32$, PA = 179° for the primary).

The $V - I$ colour map on the same scale reveals a jet-like structure elongated along PA = 119° which is similar to the UV/red biconical feature at PA = 124° (Pogge and DeRobertis, 1993). At the same time this direction is close to the [OIII] major axis at PA = 116° on the same scale (Haniff *et al.*, 1988; Pogge and DeRobertis, 1995) as well as to the triple radio source axis at PA = 125° (Ulvestad and Wilson, 1984). The secondary stellar bar axis (PA = 96°) is loosely related to the [OIII] emission (PA = 116°) and the linear radio source (PA = 125°).

The galaxy has been previously classified as (R)SAB(rs)0+: in RC3. Our V and I images show a faint outer ring, an inner ring and spiral arm-like structures at $10''$ radius in agreement with RC3.

3.5 Mkn 744 = NGC 3786

This is another example of a double-barred galaxy. The primary bar is clearly revealed as the maximum in the ellipticity curve at the $25''$ distance with $e = 0.62$ and PA = 58°. The distinct bump at the $7''$ radius indicates the presence of a secondary bar with $e = 0.29$ and PA = 75°.

The galaxy has been previously classified as SAB(rs)a pec in RC3. Out V and R images clearly show the inner ring as well as the outer ring.

3.6 Mkn 955

This galaxy has been previously classified as doubtful spiral (S?) in RC3 and as (R)SBab in MCG. Our V and I images clearly show the presence of a spiral structure, a faint outer ring and an inner ring which has not been reported previously. The maximum in the ellipticity curve at the $15''$ distance indicates the presence of a bar with $e = 0.62$ and PA = 110°.

3.7 Mkn 1058

This galaxy has been previously classified as doubtful spiral (S?) in RC3 and as uncertain barred spiral (SB:) by Markarian *et al.* (1977). Our V and I images clearly show the presence of the spiral structure. The position angle rotates from PA = 103° in the inner region to PA = 119° at the outer isophote. The presence of the bar is distinctly revealed as the maximum in the ellipticity curve at the 12″ distance with $e = 0.53$ and PA = 103°.

3.8 Mkn 1066

This galaxy is another possible example of a double–barred system. The large–scale primary bar is clearly revealed as the maximum in the ellipticity curve at the 15″ distance with $e = 0.61$ and PA = 142°. The bump at the 3" distance makes it possible to suppose the presence of a secondary bar with $e = 19$ and PA = 113°.

The primary bar is approximately aligned with the [OIII] image elongated along PA = 131° (Haniff *et al.*, 1988; Mulchaey *et al.*, 1995; Bower *et al.*, 1995) and is quite close to the triple radio source axis at PA = 134° (Ulvestad and Wilson, 1989).

This galaxy has been previously classified as (R)SB(s)0+ in RC3. The outer ring is clearly seen on the V image and slightly visible and incomplete in the I band.

3.9 Mkn 1073

This galaxy has been previously classified as (R′)SB(s)b in RC3. Both V and I images clearly show the outer ring structure. The bar is distinctly revealed as the maximum in the ellipticity curve at the 12″ distance with $e = 0.67$ and PA = 80°. In the V band there is a local maximum at the 2.3″ distance with $e = 0.22$ and PA = 100° but the I band does not show a similar feature. The $V - I$ colour map reveals the jet–like structure elongated at PA = 120° which is quite different from the bar direction.

3.10 Mkn 1157 = NGC 591

This galaxy has been not previously classified as having an inner ring ((R′)SB0 in RC3). Our images in both bands clearly show the inner ring structure as well as the outer ring.

The maximum in the ellipticity curve at the 15″ distance shows the presence of the bar with $e = 0.63$ and PA = 94°. The [OIII] emission–line image is elongated along PA = 150° (Mulchaey *et al.*, 1995). The radio map shows a double source with major axis at PA = 152° (Ulvestad and Wilson, 1989). These directions are quite different from the bar orientation.

3.11 NGC 1019

This galaxy has been previously classified as SB(rs)bc in RC3 but our images do not show any signs of an inner ring structure. The prominent bar is revealed in both

bands as the maximum in the ellipticity curve at the 10″ distance with e = 0.49 and $PA = 30°$.

3.12 NGC 3185

This galaxy is a possible example of a double–barred system. The large–scale primary bar is revealed as the maximum in the ellipticity curve at the 30″ distance with $e = 0.57$ and PA = 113°. A local maximum at the 2.3″ distance indicates the presence of the secondary bar with $e = 0.21$ and PA = 134°.

The galaxy has been previously classified as (R)SB(r)a in RC3 but there is no indication of the presence of an inner ring on our images. The outer ring structure is clearly in both bands.

3.13 UGC 524

This galaxy has been not previously classified as having an inner ring ((R′)SB(s)b in RC3). Our images in both the V and I bands clearly show the inner ring structure as well as the outer ring.

The bar is revealed as a local maximum in the ellipticity curve at the 9″ distance with $e = 0.48$ and PA = 139°. Another maximum is the result of a combination of the isophotes of the bar and outer ring.

3.14 UGC 3223

This galaxy has not been previously classified as having an inner or an outer ring (SBa in RC3). Our V image clearly shows the inner ring as well as the outer ring structures. In the I band the inner ring is hardly visible and there are only faint hints of the outer ring.

The local maximum in the ellipticity curve at the 5″ distance indicates a bar with $e = 0.50$ and PA = 72°. The global maximum is a consequence of a combination of the isophotes of the inner ring and spiral arms.

3.15 UGC 3995

This galaxy has not been previously classified as barred (S pec in RC3). Our images in both the V and I bands clearly show the bar which is revealed in the ellipticity curve as a bump at the 15″ distance with $e = 0.51$ and PA = 116°. The global maximum is the result of an isophote perturbation caused by the companion galaxy.

4 SUMMARY

In this section we summarize the results of V and I/R CCD imaging of 15 Seyfert galaxies.

One clear and one possible unidentified bar has been found in two galaxies not previously classified as barred (UGC 3995 and Mkn 530). The presence of the bar has also been confirmed in four galaxies with uncertain classification (Mkn 3, Mkn 533, Mkn 955 and Mkn 1058). Mkn 955 has been confirmed as an outer ringed galaxy as well.

Four inner rings (Mkn 955, Mkn 1157, UGC 524 and UGC 3223) and two outer rings (Mkn 744 and UGC 3223) have been found in galaxies not previously classified as having these structures. Three galaxies (Mkn 533, NGC 1019 and NGC 3185) previously classified as having inner rings did not reveal these.

For each galaxy in this paper elliptical fits to isophotes have been made and the position angles and the axial ratios of the bars and the outer contours have been obtained. As a result four multiple–barred galaxies have also been found. Mkn 573 and Mkn 744 distinctly show a secondary bar within a primary bar. Mkn 1066 and NGC 3185 have been classified as possible double–barred galaxies (i.e. having bars within bars).

The bar orientations have been compared with the [OIII] and radio major axes for five objects with known [OIII] and radio maps. It has been determined that the bar is aligned with the [OIII] and radio emission in Mkn 533, Mkn 573 and Mkn 1066. In Mkn 3 and Mkn 1157 the large–scale bar is unrelated to the [OIII] image or with the radio source.

It has been found that the colour maps of Mkn 3, Mkn 573 and Mkn 1073 show jet–like structures in the inner regions. In Mkn 3 and Mkn 573 these features are similar to the [OIII] images on the same scale and have position angles close to those of the radio sources.

Acknowledgements

This research was supported by the Russian Foundation of Fundamental Research through grant number 96–02–16409a and the Russian Federal Science–Technical Programme "Astronomy" through grant 2–58.

We are very grateful to V. V. Vlasyuk for providing image processing and elliptical-fitting programs and for help with the data reduction, and V. R. Amirkhanian for help with the observations. We are especially grateful to S. N. Dodonov and the laboratory of spectroscopy and photometry of extragalactic objects for the comprehensive support of this work.

References

Adams, T. F. (1977) *Astrophys. J. Suppl.* **33**, 19.

Afanasiev, V. L., Dodonov, S. N., Borisenko, A. N., Markelov, S. V., and Rjadchenko, V. P. (1991) Prepr. SAO AS, No. 76.

Afanasiev, V. L., Fridman, A. M., and Pasha, I. I. (1987) Proc. 10th European Regional Meeting of the IAU **4**, 319.

Afanasiev, V. L. and Kostiuk, I. P. (1996) In *Barred Galaxies*, Astronomical Society of the Pacific Conference Series **91**, 233.

Afanasiev, V. L. and Sil'chenko, O. K. (1991a) *Astrofiz. Issled. (Izv. SAO)* **33**, 88, (I).

Afanasiev, V. L. and Sil'chenko, O. K. (1991b) *Astrofiz. Issled. (Izv. SAO)* **33**, 104, (II).
Afanasiev, V. L. and Sil'chenko, O. K. (1991c) *Astrofiz. Issled. (Izv. SAO)* **33**, 114, (III).
Afanasiev, V. L. and Sil'chenko, O. K. (1991d) *Astrofiz. Issled. (Izv. SAO)* **33**, 125, (IV).
Afanasiev, V. L. and Sil'chenko, O. K. (1991e) *Astrofiz. Issled. (Izv. SAO)* **33**, 132, (V).
Afanasiev, V. L. and Sil'chenko, O. K. (1991f) *Astrofiz. Issled. (Izv. SAO)* **33**, 144, (VI).
Arp, H. (1971) *Astrophys. J. Lett.* **7**, 221.
Bender, R. and Möllenhoff, C. (1987) *Astron. Astrophys.* **177**, 71.
Bower, G., Wilson, A. S., Morse, J. A., Gelderman, R., Whittle, M., and Mulchaey, J. (1995) *Astrophys. J.* **454**, 106.
Capetti, A., Macchetto, F., Axon, D. J., Sparks, W. B., and Boksenberg, A. (1995) *Astrophys. J.* **448**, 6.
Christian, C. A., Adams, M., Barnes, J. V., Butcher, H., Hayes, D. S., Mould, J. R., and Siegel, M. (1985) *Pub. Astron. Soc. Pac.* **97**, 363.
de Vaucouleurs, G., de Vaucouleurs, A., Corwin, H. G., Buta, R. J., Paturel, G., and Foque, P. (1991) *Third Reference Catalogue of Bright Galaxies*, New York, Springer, RC3.
Granato, G. L., Zitelli, V., Bonoli, F., Danese, L., Bonoli, C., and Delpino, F. (1993) *Astrophys. J. Suppl.* **89**, 35.
Haniff, C. A., Wilson, A. S., and Ward, M. J. (1988) *Astrophys. J.* **334**, 104.
Landolt, A. U. (1992) *Astron. J.* **104**, 340.
Lipovetsky, V. A., Neizvestny, S. I., and Neizvestnaya, O. M. (1987) *Soobshch. Spec. Astrofiz. Obs. of AS USSR* **55**, 5.
MacKenty, J. W. (1990) *Astrophys. J. Suppl.* **72**, 231.
McLeod, K. K. and Rieke, G. H. (1995) *Astrophys. J.* **441**, 96.
Markarian, B. E., Lipovetsky, V. A., and Stepanian, J. A. (1977) *Astrofizika* **13**, 225.
Márquez, I. (1996) In *Barred Galaxies*, Astronomical Society of the Pacific Conference Series **91**, 212.
Mikhailov, V. P. (1986) *Soobshch. Spec. Astrofiz. Obs. of AS USSR* **50**, 71.
Moles, M., Márquez, I., and Pérez, E. (1995) *Astrophys. J.* **438**, 604.
Mulchaey, J. S., Wilson, A. S., and Tsvetanov, Z. (1995) STSI prepr., No. 973.
Pogge, R. W. and De Robertis, M. M. (1993) *Astrophys. J.* **404**, 563.
Pogge, R. W. and De Robertis, M. M. (1995) *Astrophys. J.* **451**, 585.
Sharp, N. A. (1986) *Astrophys. J.* **302**, 245.
Shlosman, I., Frank, J., and Begelman, M. C. (1989) *Nature* **338**, 45.
Shuder, J. M. and Osterbrock, D. E. (1981) *Astrophys. J.* **250**, 55.
Simkin, S. M., Su, H. J., and Schwarz, M. P. (1980) *Astrophys. J.* **237**, 404.
Ulvestad, J. S. and Wilson, A. S. (1984) *Astrophys. J.* **278**, 544.
Ulvestad, J. S. and Wilson, A. S. (1989) *Astrophys. J.* **343**, 659.
Unger, S. W., Pedlar, R. V., Booler, R. V., and Harrison, B. A. (1986) *Mon. Not. Roy. Astron. Soc.* **219**, 387.
Vorontsov–Vel'yaminov, B. A., Krasnogorskaja, A. A. (1962–1968) *Morphological Catalog of Galaxies, I-IV*, Moscow State University, Moskow, (MCG).
Wilson, A. S., Pooley, G. G., Willis, A. G., and Clements, E. D. (1980) *Astrophys. J. Lett.* **237**, L61.
Wilson, A. S., Ward, M. J., and Haniff, C. A. (1988) *Astrophys. J.* **334**, 121.
Yee, H. K. C. (1983) *Astrophys. J.* **272**, 473.